

# **Hydrogeology of the Boulder River Watershed Study Area and Examination of the Regional Ground-Water Flow System Using Interpreted Fracture Mapping from Remote Sensing Data**

By Robert R. McDougal, M.R. Cannon, Bruce D. Smith, and David A. Ruppert

Chapter D9 of

**Integrated Investigations of Environmental Effects of Historical  
Mining in the Basin and Boulder Mining Districts, Boulder River  
Watershed, Jefferson County, Montana**

Edited by David A. Nimick, Stanley E. Church, and Susan E. Finger

Professional Paper 1652–D9

**U.S. Department of the Interior  
U.S. Geological Survey**

# Contents

Abstract .....	341
Introduction .....	341
Purpose and Scope .....	343
Hydrogeologic Setting .....	343
Elkhorn Mountains Volcanics .....	343
Boulder Batholith .....	344
Tertiary Volcanics .....	344
Unconsolidated Deposits .....	344
Ground-Water Recharge and Discharge.....	345
Methods of Investigation.....	345
Conceptual Model of Ground-Water Flow.....	345
Linear Feature Mapping .....	345
Results and Analysis .....	352
Conceptual Model of Ground-Water Flow.....	352
Linear Feature Analysis .....	354
Conclusions and Discussion .....	361
References Cited .....	368

# Figures

1. Site map for hydrogeologic study of the Boulder River watershed .....	342
2. Landsat 5 scene comparing unfiltered band 4 with image filtered to enhance northeast-trending features.....	346
3. Landsat 5 scene to which a principal components transformation was applied, and directionally filtered to enhance northeast-trending linear features .....	348
4. IRS-1C panchromatic satellite image directionally filtered and bit error filter applied .....	349
5. Shaded relief Digital Elevation Model images showing illumination from two different directions .....	350
6. Site map showing 7.5-minute quadrangle boundaries, linear feature mapping quadrants, and approximate area of the Butte-Helena fault zone.....	351
7. Conceptual ground-water model and depiction of flow regimes.....	353
8. Map showing linear features, Boulder River watershed study area.....	357
9. Rose diagrams representing orientations of all linear features and all linear features weighted by length .....	358
10. Length filtered rose diagrams of linear features in several ranges of lengths .....	359
11. Rose diagrams showing linear feature orientation arranged by quadrants shown in figure 6.....	360

12–17. Contour maps of:	
12. Linear feature spatial frequency.....	362
13. Linear feature length.....	363
14. Linear feature intersections .....	364
15. Combined linear feature spatial frequency and intersections .....	365
16. Combined linear feature spatial frequency and total length.....	366
17. Combined linear feature spatial frequency and intersections, and areas of mapped shallow ground water.....	367

## Tables

1. Summary statistics for mapped linear features .....	354
2. Summary statistics for orientations of mapped linear features .....	355
3. Summary of main orientations of mapped linear features .....	356

## ***Chapter D9***

# **Hydrogeology of the Boulder River Watershed Study Area and Examination of the Regional Ground-Water Flow System Using Interpreted Fracture Mapping from Remote Sensing Data**

By Robert R. McDougal, M.R. Cannon, Bruce D. Smith, and David A. Ruppert<sup>1</sup>

### **Abstract**

This investigation describes the shallow unconsolidated and upper fracture-controlled ground-water flow regimes in the Boulder River watershed, and uses remote sensing data to map linear surface features that are interpreted as fractures and are assumed to be associated with regional fracture controlled subsurface flow. Ground water in the Boulder River watershed occurs primarily in saturated unconsolidated deposits and the upper portion of a fractured bedrock aquifer. The hydraulic properties of the bedrock aquifer, at depth, are largely unknown. However, along fault zones, mineralized zones, and some large fractures, the hydraulic conductivity may be significant. A conceptual model of ground-water flow was developed based on hydrogeologic characteristics of aquifers investigated near the inactive Buckeye, Bullion, and Crystal mines, and on observations of ground-water discharge from granitic, volcanic, and unconsolidated rock units throughout the Basin Creek and Cataract Creek drainages. The direction of shallow ground-water flow can be modeled as the gradient of topographic slope. Deeper ground-water flow likely is a function of fracture width, continuity, and interconnectivity, and likely is partly controlled by the heterogeneous and anisotropic orientation of fractures. Four remote sensing data sets, used as base images, provided a range of spatial resolutions for linear feature mapping. Endpoint data from mapped linear features, used in a 2-D orientation analysis, enabled us to determine primary orientations of lineaments from rose diagrams and to produce contour maps of linear feature characteristics. A contour map of combined linear feature spatial frequency and intersections was compared with a map of wetland-soils areas to identify correlated areas of high fracture occurrence and areas where the potentiometric surface is close to the land

surface. The mapped lineaments show a consistent east-west primary orientation. The greatest linear feature spatial frequency, length, and frequency of intersections occurred on the Continental Divide at the northern boundary of the Boulder River watershed study area. The observation of highest interpreted fracture frequency on the Continental Divide is significant in that this area may provide potential recharge for fracture-controlled ground water. The comparison of highest interpreted fracture frequency with areas of mapped shallow ground water shows a correlation in several locations between potential areas of recharge to the fractured granitic aquifer and areas of discharge, or wet soils. The description of the ground-water regime and the identification of areas of high interpreted fracture frequency are components of the ground-water system that should be considered in the design of strategies for mine remediation.

### **Introduction**

The Boulder River watershed is representative of mountainous terrains in the western United States where ground water occurs in unconsolidated Quaternary alluvial and colluvial deposits, and in fractures in underlying plutonic rocks. The crystalline bedrock aquifers commonly have significantly lower hydraulic conductivity and storage potential than the unconsolidated aquifers, except where substantial secondary fracture permeability exists.

Based on field observations near the inactive Buckeye, Bullion, and Crystal mines, and on observations of ground-water discharge from granitic, volcanic, and unconsolidated rock units throughout the Basin Creek and Cataract Creek drainages (fig. 1), the hydraulic characteristics and flow regimes of the upper part of the ground-water system in the Boulder River watershed are relatively well understood. The hydraulic properties of the fractured bedrock aquifer and its

---

<sup>1</sup>United States Department of Agriculture (USDA) Forest Service, Beaverhead-Deerlodge National Forest, Butte, Mont.

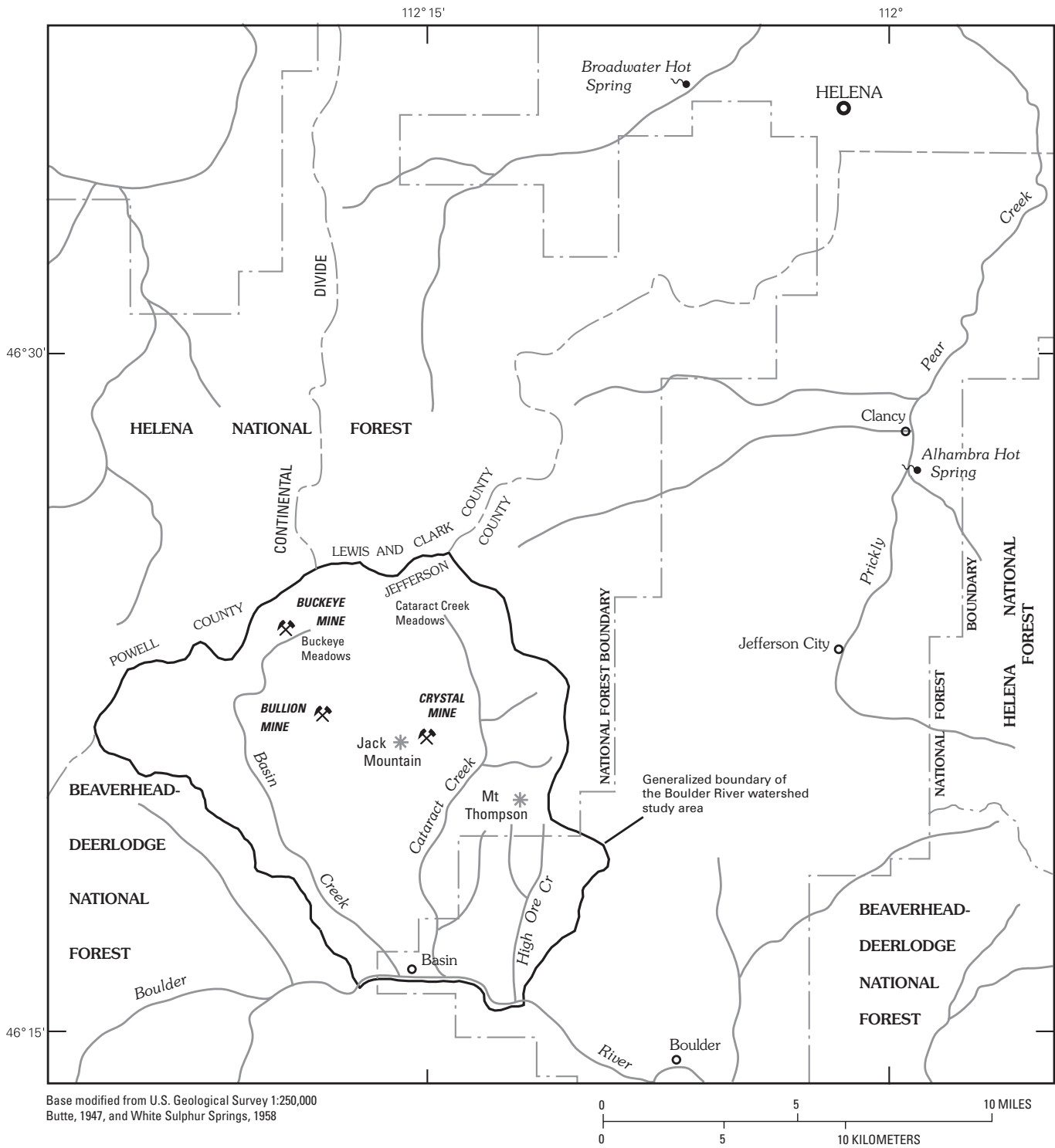


Figure 1. Site map for hydrogeologic study of the Boulder River watershed.

contribution to the regional ground-water system, however, have not been well characterized. Similarly, the relative importance of shallow (local) and deep (regional) ground-water flow as pathways for transporting metals from mining-related and natural sources to streams in the watershed is not well understood. Detailed synoptic streamflow measurements indicated that ground water discharges to streams in several locations in the study area (Kimball and others, this volume, Chapter D6).

This investigation describes the shallow unconsolidated, and upper fracture-controlled ground-water flow regimes within the Boulder River watershed study area, and uses remote sensing data to map linear surface features in approximately 528 mi<sup>2</sup> of the watershed and surrounding area. The mapped linear features identified in this study are interpreted to represent the surface expression of faults, joints, and other fractures in the Butte pluton and overlying volcanic rocks. The regional and subregional structurally controlled ground-water flow regimes are assumed to be associated with the orientation of these linear features.

Previous studies have shown that mineral deposits and hydrothermal fluid flow in many mining districts occur along linear trends that can range in length from tens of feet to tens of miles in length (Rowan and Wetlaufer, 1975). Remote sensing data, such as Landsat Thematic Mapper (TM) data, have successfully been used to evaluate the relationship between mineral deposits and linear structural features (Sabins, 1987). Concepts from these previous studies have been applied in this study to examine the potential relation between fracture systems and ground-water flow. The statistical analysis of linear feature orientation presented here is intended to provide a general view of the potential regional flow directions in the bedrock aquifer by identifying primary azimuths of mapped linear features. To identify and map all structural features from remotely sensed data is not possible, because of ground resolution limitations, vegetation cover, and alluvial or colluvial cover. It is also not possible, in most cases, to differentiate types of linear features. That is, is the linear feature the surface expression of a fault, fracture, joint, or mineralized vein? Mapped linear features from these data sets provide a representation of the spatial distribution and orientation of bedrock fractures, and that of fractures in overlying volcanic rocks. Therefore, maps of this type should be interpreted as a statistical sample of the naturally occurring linear features in a region (Knepper, 1996).

## Purpose and Scope

The purpose of this investigation is to provide a conceptual representation of the ground-water system in the Boulder River watershed study area. The objectives of the study are to

- Develop a conceptual model of ground-water flow for the purpose of describing the relative magnitude of ground-water flow systems in various rock units.

- Map linear features from remote sensing imagery. The linear features are assumed to represent the spatial distribution, spatial frequency, and orientation of faults, joints, and fractures associated with structurally controlled ground-water flow.
- Compare a contour map of combined linear feature spatial frequency and intersections with a wet soils coverage representing areas of inferred shallow ground water. Areas that have high fracture frequency and wet soils may be areas of recharge or discharge for fracture-controlled ground-water flow.
- Evaluate how the ground-water flow systems may affect mine-site remediation in the watershed.

## Hydrogeologic Setting

Igneous rocks of the Cretaceous Elkhorn Mountains Volcanics and cogenetic Boulder batholith, and Tertiary volcanic rocks, crop out over most of the Boulder River watershed study area and adjacent areas (O'Neill and others, this volume, Chapter D1). In places, the igneous rocks are overlain by unconsolidated surficial deposits of various origin, including glacial drift, stream alluvium, bog deposits, and mass-wasting deposits. Hydrogeologic characteristics of the thin and porous surficial deposits are vastly different from those of the underlying massive, low-permeability igneous rocks. Characteristics such as permeability, fracture density, degree of weathering, and thickness and extent of geologic units have a major control on location and magnitude of ground-water flow systems in the region.

### Elkhorn Mountains Volcanics

The Elkhorn Mountains Volcanics are present on many of the higher ridges and peaks in the northwestern part of the study area, on Jack Mountain in the central part of the study area, and in the Mount Thompson area near the headwaters of High Ore Creek. Primary permeability of the volcanic rocks is very low; however, where the rocks were examined on Jack Mountain and in the northern part of the Basin Creek drainage, they were highly fractured with many open and intersecting fractures. Samples of Elkhorn Mountains Volcanics collected on Jack Mountain by Desborough and others (1998) were intensely fractured at intervals of about 4 in. or less and were silicified. Core holes drilled on Jack Mountain (Maxim Technologies, Inc., 1999) revealed that fractures in the subsurface generally were clay filled, and a slug test in one of the holes indicated a hydraulic conductivity of 0.3 ft/day. Nearly all hydraulic conductivity of the volcanic rocks is a result of the intense fracturing. Based on observed fracture systems, the Elkhorn Mountains Volcanics in the northern and central parts of the study area have small ground-water storage capacity with low to moderate hydraulic conductivity, largely dependent on the degree of clay filling in the fractures.

## Boulder Batholith

Plutonic, granodioritic rocks of the Butte pluton of the Boulder batholith underlie most of the study area and extend for many miles beyond the study area boundary. Nearly all permeability of the Butte pluton is the result of fracturing and near-surface weathering. Plutonic rocks in outcrop generally are highly fractured and have three prominent sets of closely spaced joints. Observations of nearly 500 joints in the plutonic rocks documented a prominent joint set that trends about east and dips steeply north, a set that trends about north and most commonly dips steeply west, and a set that trends east and most commonly dips gently south (Ruppel, 1963). The joints are spaced from a few inches to many feet apart. In the Basin 7.5-minute quadrangle, the north-trending steep joints are from about 1 to 5 ft apart and the east-trending steep joints are from 5 to 10 ft apart. Individual joints are rarely more than 30 ft long, but where one joint dies out it commonly is overlapped by a parallel joint that is entirely separate or that is connected by a linking transverse joint (Ruppel, 1963).

Outcrops of the Butte pluton are characterized by large open fractures caused by weathering along existing joints (O'Neill and others, this volume, fig. 11). In many areas, joints in the rocks have sufficiently weathered to leave large, free-standing, rounded boulders. Weathering of the plutonic rocks decreases rapidly with depth, which is clearly evident in many road cuts, mine workings, excavations, and drill holes. In areas examined, the upper 5 ft of rock typically contain open joints. From about 5 to 50 ft in depth, the plutonic rock grades from slightly weathered to unaltered rock; most joints become tight; and many are filled with clay. Below about 50 ft, rocks of the Butte pluton typically are fractured, although most fractures are extremely tight, and weathering is observed only on some fracture surfaces. Exceptions to these general characteristics are found along fault zones, mineralized zones, and some large fractures.

Hydraulic conductivity of the granodioritic rocks of the Butte pluton typically is very low. At a core hole drilled south of the Bullion mine, hydraulic conductivity measured from a slug test was about 0.02 ft/day (Maxim Technologies Inc., 1999). At another core hole on the Continental Divide 2.5 mi north of the study area, the hydraulic conductivity of the plutonic rocks was about 0.04 ft/day, as determined from a slug test (Maxim Technologies Inc., 1999). Water wells drilled into the granodioritic rocks typically have small yields, although well yields are highly variable and range from 0 to as much as 100 gallons per minute (Montana Department of Natural Resources and Conservation, unpublished data). Well yield is highly dependent on degree of fracturing and connection of the fractures to sources of recharge.

## Tertiary Volcanics

Tertiary volcanic rocks are present in relatively small areas of the Boulder River watershed study area and include

quartz latite of Eocene age and rhyolite of Oligocene-Eocene age. Quartz latite of the Lowland Creek Volcanics is present in several small outcrops near the town of Basin; rhyolitic rocks crop out near the Continental Divide in the northwestern part of the study area (O'Neill and others, this volume). Most of the joints in the Tertiary volcanic rocks are primary joints and partings resulting from flowage and cooling (Ruppel, 1963). Columnar joints are common in outcrops of rhyolite and quartz latite welded tuff. Platy jointing parallel to flow laminae is common in rhyolite and results in weathered outcrops that have the appearance of rock rubble. Typically, the permeability and hydraulic conductivity of these types of volcanic rocks are relatively low (Freeze and Cherry, 1979). However, in areas where fracturing occurs, there can be a wide range of secondary permeability that largely is dependent on the degree of fracturing and amount of clay in fractures.

## Unconsolidated Deposits

Unconsolidated deposits, consisting chiefly of Quaternary glacial deposits and stream alluvium, mantle a large part of the bedrock surface in the upper valleys of Basin Creek and Cataract Creek. Glacial deposits in the study area include bouldery till, outwash, and lake sediments, with till being by far the most abundant (O'Neill and others, this volume). The glacial deposits are reported to be early Wisconsin in age, equivalent to the Bull Lake stage of glaciation in the Wind River Mountains of Wyoming (Ruppel, 1963). Other young unconsolidated deposits include small areas of colluvium, talus, landslide, and bog deposits. Thickness of unconsolidated deposits ranges from less than 1 ft to more than 31 ft in some stream valleys as observed in road cuts and drill holes in the study area.

In the northwest part of the study area, arkosic sand and silt deposits underlie Oligocene-Eocene volcanic rocks, with weakly consolidated early Tertiary sedimentary rocks also present. Due to the weakly consolidated character of these rocks, anomalous hydrologic conditions exist along the Continental Divide at the base of the rhyolitic volcanic rocks. Unusually moist and wet soil conditions associated with bogs and springs are typical along the base of the rhyolitic volcanics (O'Neill and others, this volume).

Most surficial unconsolidated deposits are fairly thin, whereas the weakly consolidated Tertiary deposits may be as much as 45 ft thick. These deposits are important local aquifers because of their relatively large hydraulic conductivity and porosity. All of these deposits are readily recharged by precipitation, and many small springs and seeps discharge from unconsolidated deposits near or along their contact with underlying bedrock. Discharge from the springs typically varies from peak flow in the spring or early summer to low flow or no flow by late summer. These flow characteristics are typical of springs fed by local ground-water flow systems. Hydraulic conductivity of unconsolidated deposits, measured from slug tests at nine wells near the Buckeye mine, ranged

from 0.03 to 40 ft/day, with a median of 0.2 ft/day (Cannon and others, this volume, Chapter E1, table 5). The lowest measured hydraulic conductivity values were in till; the highest value was in alluvial sand.

## Ground-Water Recharge and Discharge

Recharge to aquifers primarily occurs from snowmelt and large precipitation events in spring and early summer. Recharge likely occurs on most topographic highs, and greater amounts of recharge are in areas with the highest precipitation and highest hydraulic conductivity. The water table is near land surface in much of the study area, including high-elevation ridges and slopes, as observed from wells and springs. Discharge in the form of numerous small springs and seeps occurs in topographic lows, at abrupt breaks in slope, and at geologic contacts where there is a downward decrease in hydraulic conductivity. Ground-water flow paths in the upper aquifers, from recharge to discharge areas, are generally short—commonly less than a few thousand feet. Most active ground-water circulation occurs in unconsolidated deposits and the upper 50 ft of fractured bedrock.

Nearly all discharges observed in mine workings, road cuts, exploration pits, and natural springs were characterized as discharge from local ground-water flow systems based on characteristics such as topographic position, seasonal variation in flow, water quality, and geologic source. Water contained in fractures within the upper 50 ft of plutonic rocks generally is part of the local ground-water flow system and, on a macroscopic scale, flow direction in the rock is likely controlled largely by topography.

Discharge from regional flow systems was not observed within the study area. A very small part of annual recharge likely enters deep, regional flow systems through some fault and large fracture zones. Regional ground-water flow would be constrained by the very low hydraulic conductivity of the granodioritic bedrock, and would occur only as the result of secondary permeability along faults and fractures. Direction of flow within the regional system is presumably controlled by geologic structure and topography. Possible discharge areas for regional flow originating in the study area are Broadwater hot springs on the north end of the Butte pluton west of Helena and the Prickly Pear Creek valley east of the study area, in the vicinity of Alhambra hot springs (fig. 1).

Base-flow discharge of streams that drain the study area is sustained by ground-water flow from unconsolidated deposits and the upper zone of fractured and weathered bedrock. The small ground-water discharge available from the shallow aquifers and the lack of regional ground-water discharge to the streams are evident in the small base flow and steep recession curves of stream hydrographs (Church, Nimick, and others, this volume, Chapter B, fig. 3). Base flow of Basin Creek, Cataract Creek, and High Ore Creek, determined from winter measurements made from 1996 to 2000, averaged 0.11 ft<sup>3</sup>/s from each square mile of drainage area. The base-flow discharge is equivalent to 1.5 in. of runoff per year from the entire drainage area.

## Methods of Investigation

### Conceptual Model of Ground-Water Flow

Theoretical and mathematical ground-water flow concepts documented by Hubbert (1940), Toth (1963), and Freeze and Witherspoon (1966, 1967) form the basis of modern ground-water modeling. Data requirements for model development include (1) hydraulic conductivity distribution of the geologic units within the drainage basin, (2) geometry of the basin, including variations in topography and location of basin boundaries, and (3) configuration of the water table as determined from measurements of water levels in wells and by the measurement of elevation of recharge and discharge areas. A conceptual model of steady-state ground-water flow in the Boulder River watershed was constructed through the application of theoretical ground-water flow concepts to observed hydrogeologic properties of rocks and topographic and hydrologic characteristics of the study area. Included in the model are representations of typical flow regimes within the watershed.

### Linear Feature Mapping

Four data sets, Landsat Thematic Mapper (TM), India Remote Sensing satellite (IRS 1-C) panchromatic, U.S. Geological Survey Digital Orthophoto Quads (DOQ), and U.S. Geological Survey Digital Elevation Models (DEM), were used to generate base images for mapping linear features. The different spatial resolutions of these data sets facilitated identification of linear features at various scales, ranging in length from a few hundred feet to several miles. All image processing and enhancement was performed using ENVI® (Environment for Visualizing Images, Research Systems Inc., 1998).

Images produced from the Landsat TM data<sup>2</sup> (94 ft (30 m)<sup>3</sup> spatial resolution) were processed to enhance linear surface features by applying directional convolution filters to the images to emphasize north-south-, east-west-, northeast-southwest-, and northwest-southeast-trending linear features, and features adjacent to these principal directions (fig. 2). In all of the images where directional filters were used (TM, IRS, and DOQ), a user-defined addback value of 75 percent of the original image was selected. A principal components (PC) transformation was applied to maximize the variance of the TM multispectral data. This process is useful for identifying less correlated information in the data set which may

<sup>2</sup>The Landsat 5 scene was obtained from EROS Data Center and is part of the Multi-Resolution Land Characteristics (MRLC) data set. Entity ID number: MBP03902806281994. Image acquisition date: June 28, 1994. Path 39, row 28.

<sup>3</sup>The spatial resolution of remote sensing data is usually reported in metric units.



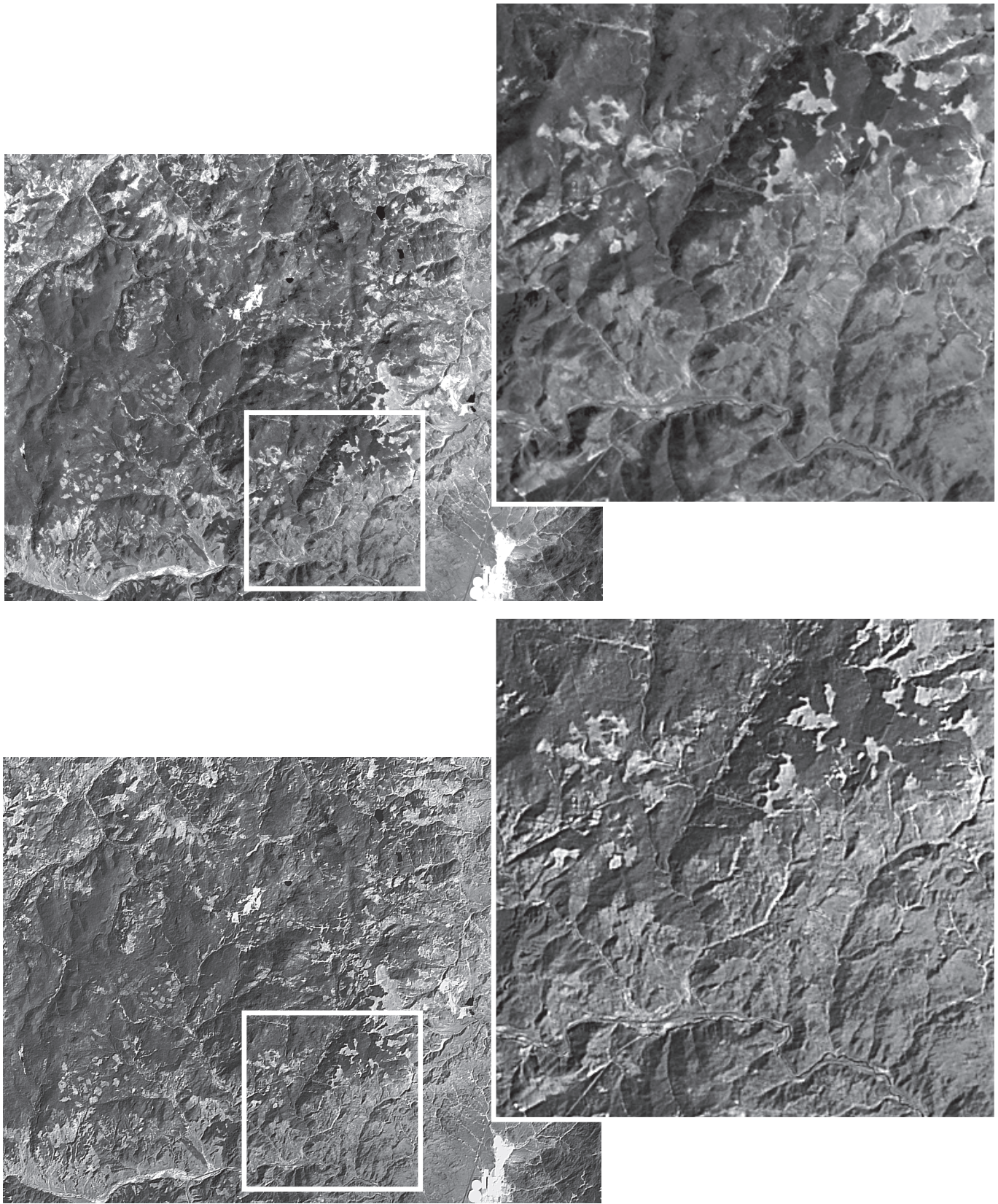


**Figure 2.** Comparison of unfiltered Landsat Thematic Mapper (TM) band 4 image (top) and TM band 4 image filtered to enhance northeast-trending features (bottom). In each image pair, the white outline is enlarged in the upper right view.

be overwhelmed by the highly correlated topographic and albedo effects (Sabins, 1987). After inspection of the six resulting principal component images, PC-3 was selected because it provided the most suitable base image for mapping. Directional filters were applied to the image, as previously described, to enhance linear features (fig. 3). Lineaments considered to represent faults, fractures, or other geologic structures were mapped from each TM base image and included in a vector coverage. The endpoint map and image coordinates for each vector were recorded. The same mapping procedure was used for all the other data sets.

The IRS panchromatic data<sup>4</sup> (16 ft (5 m) spatial resolution) were filtered to reduce the effects of nonperiodic banding in the image. This noise is the result of sensitivity variations in the IRS satellite's "push-broom" detector array. A bit error filter (Eliason and McEwen, 1990) was used to minimize the resulting noise. The residual banding, however, could not be completely removed without degrading the image. The resulting image was directionally filtered to enhance linear features as previously described (fig. 4). Because of the northeast-southwest trend of the residual banding, the image was not used to map linear features oriented in this direction.

Six DOQ images<sup>5</sup> (3.3 ft (1 m) spatial resolution), corresponding to the 7.5-minute topographic quadrangles covering the study area, were directionally filtered as previously described. The resulting images, having the highest spatial resolution, were used to identify the smallest mappable linear features.

When linear features are mapped from satellite or aerial imagery, an important consideration is that visual bias will be introduced by the direction of solar illumination. Linear features that are oriented parallel to the direction of solar illumination are often not as easily identified as those oriented perpendicular to this direction, where shadowing becomes more prominent. To minimize this effect, a DEM (33 ft (10 m) spatial resolution) was used to produce two shaded relief images that could be artificially illuminated from any selected direction, and using any selected sun elevation angle (fig. 5). The solar illumination azimuths are 124° for the TM data, 148° for the IRS data, and 120° for the DOQ data. Based on this predominantly southeastern illumination direction of the data sets, the shaded relief images were illuminated from 0° and 45°, with a solar elevation angle of 45°.

The geographic coordinates (recorded as Universal Transverse Mercator (UTM) coordinates) of the endpoints of each mapped vector were used to calculate the azimuth and length of each linear feature. These data were used in a 2-D orientation analysis (Rockworks™, Rockware® Inc., 1999) to determine primary orientations of lineaments from rose diagrams and to produce contour maps of linear feature characteristics. Rose diagrams are polar histograms, which represent

the two-dimensional (horizontal plane) orientations of mapped linear features. The statistical parameters of sample size ( $N$ ), maximum percentage, mean percentage, vector mean azimuth (direction), standard deviation, confidence interval, and R-magnitude were calculated for each diagram. The maximum percentage is the histogram class with the greatest frequency, while the mean percentage is the class containing the average frequency. The confidence interval represents the interval on either side of the mean azimuth that most likely (using a 95 percent confidence level) contains the true mean direction. The R-magnitude values are standardized to range from 0 to 1 and are a measure of the magnitude of the azimuth mean. Data sets with a large dispersion about the mean have small values for R (values near 0), and data sets that are tightly grouped around the mean have a large value for R (values near 1).

Rose diagrams were produced to display the primary orientations of linear features. Petals in each rose diagram were either sized proportional to the length of the lineaments (total length of linear features within a 10° class range) or sized proportional to the spatial frequency of the lineaments within a 10° class range. The linear feature data were filtered using length groupings of 3.3–1,640 ft (1–500 m)<sup>6</sup>, 1,640–3,281 ft (500–1,000 m), 3,281–9,843 ft (1,000–3,000 m), and 9,843–26,247 ft (3,000–8,000 m). Length-proportional rose diagrams were produced for each length group. The length groupings are meant to compare the orientations of short, short to medium, medium to long, and long length ranges of linear features.

The northeast-trending Butte-Helena fault zone divides the study area roughly into a southeastern region of synemplaced diastrophic fractures of the Butte pluton, and a western laccolithic region (O'Neill and others, this volume). The study area was divided into four quadrants (fig. 6), and rose diagrams of linear feature spatial frequency were plotted for each quadrant. Linear features were assigned to the quadrant that contained the midpoint of the linear feature. The rose diagrams corresponding to the four quadrants are intended to illustrate differences in linear feature orientation associated with differing geologic subregions and environments.

Contour maps of the spatial frequency, length, occurrence of intersections, combined spatial frequency and intersections, and combined spatial frequency and length were produced by interpolating the linear feature data using the kriging<sup>7</sup> gridding method (Surfer 7®, Golden Software, Inc.). In a spatial frequency grid, the value assigned to each grid cell represents the number of linear features that lie in the cell. This number includes lines that originate in the cell, end in the cell, and pass through the cell. In a length grid, the value for each

<sup>6</sup>The linear feature data were originally recorded as endpoints in UTM coordinates, and the length groupings were based on calculated lengths from the metric coordinates. Therefore, metric units are also shown here.

<sup>7</sup>Kriging is a geostatistical gridding method that is often used to produce contour maps from irregularly spaced data. Kriging attempts to express trends suggested in the data by taking into account what is known about the spatial characteristics of the data (Isaaks and Srivastava, 1989).

<sup>4</sup>IRS-1C Pan Image acquired from Space Imaging Inc. path/row/section: 252/036/A & 252/036/B. acquisition date: 7-16-97(a) & 11-13-97(b).

<sup>5</sup>This data set is from the National Technical Means (NTM) declassified archives. The images, as received, have been degraded to 3.3 ft (1 m) spatial resolution.

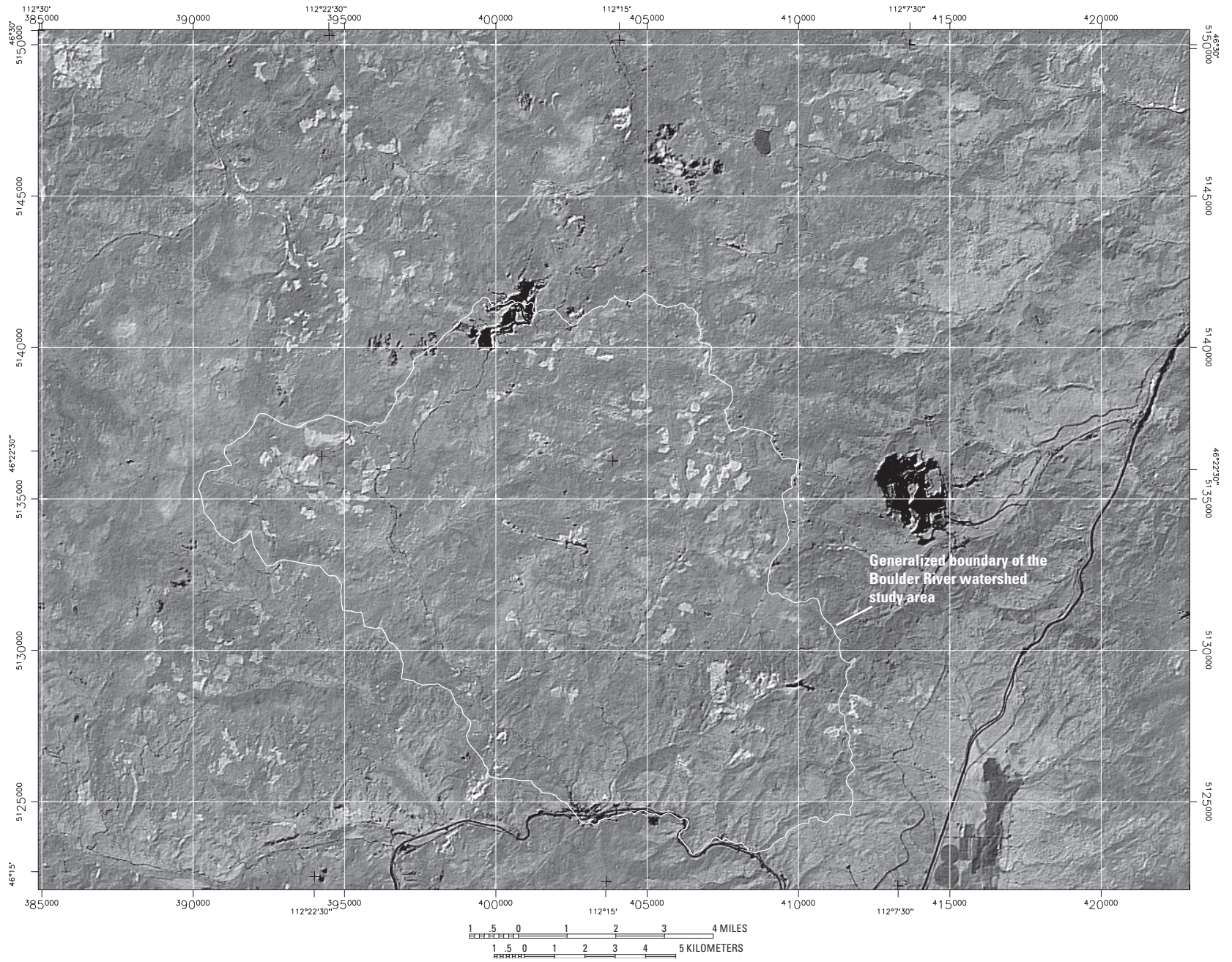


**Figure 3.** Landsat Thematic Mapper (TM) Principal Component (PC) 3, directionally filtered to enhance northeast-trending linear features.

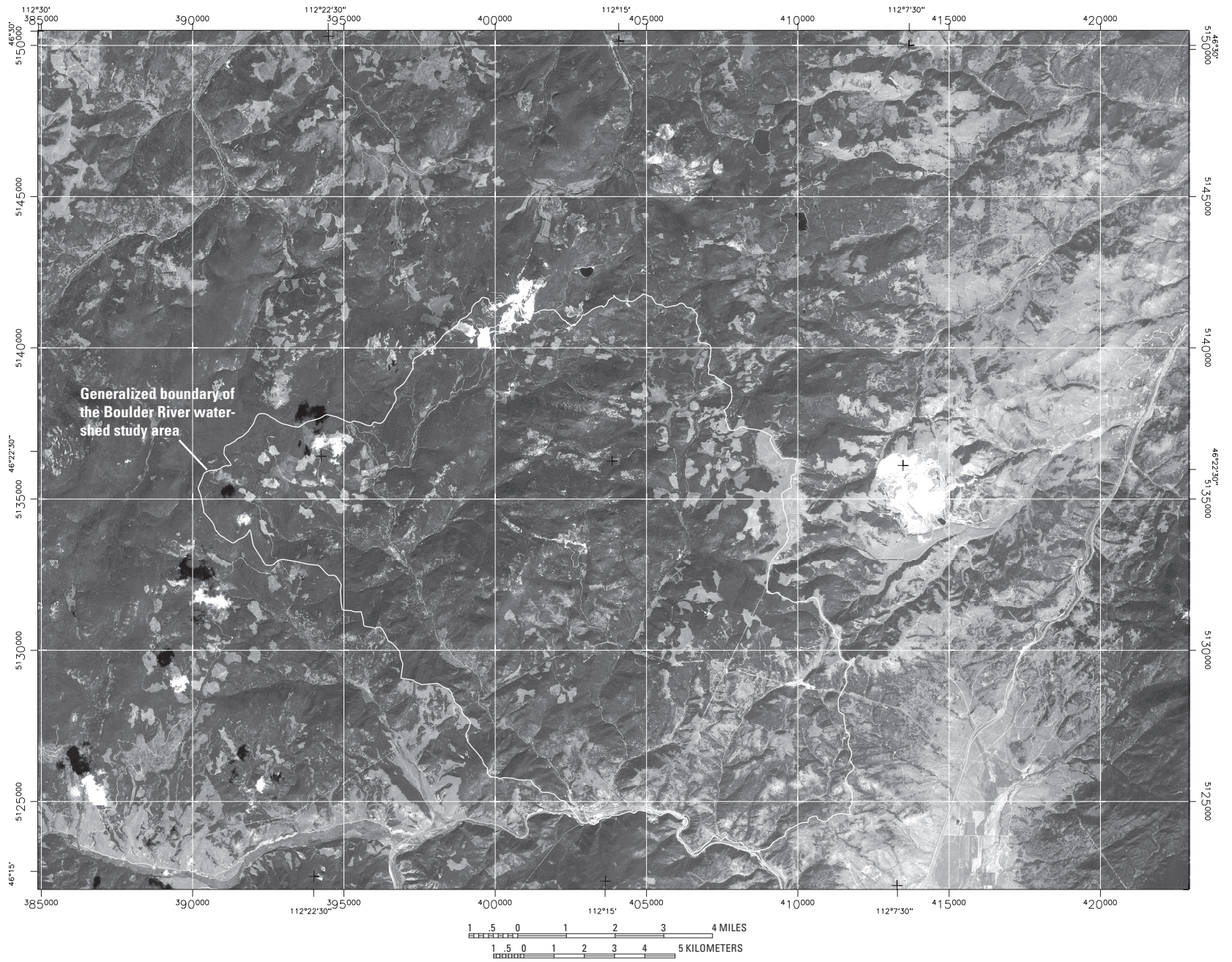


**Figure 4.** IRS-1C satellite image directionally filtered to enhance linear features and a bit error filter applied to remove residual noise (16 ft or 5 m spatial resolution).

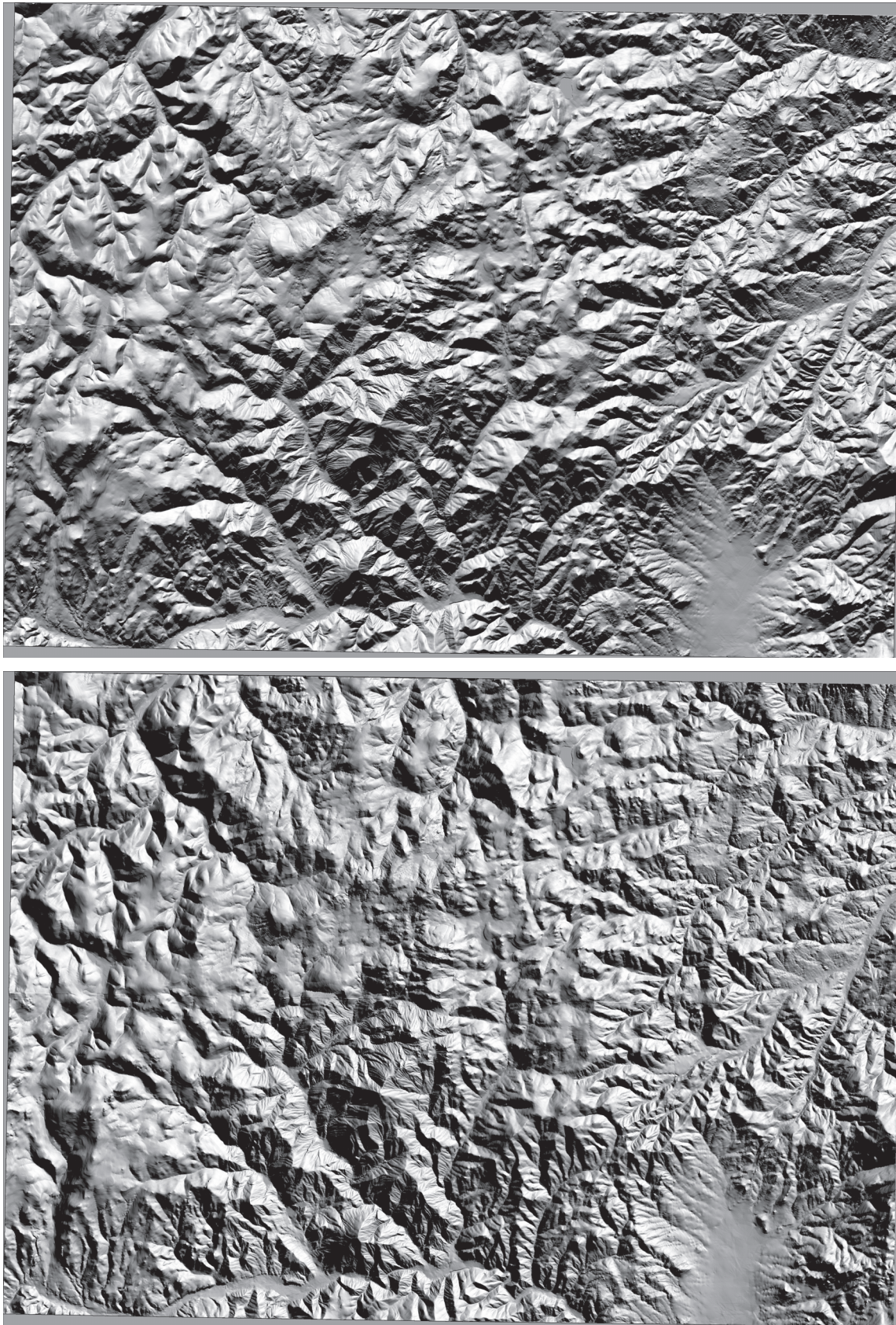


**Figure 5.** Shaded relief Digital Elevation Model (DEM) images artificially illuminated from 0° azimuth (top) and 45° azimuth (bottom) (area shown corresponds to previous figures).

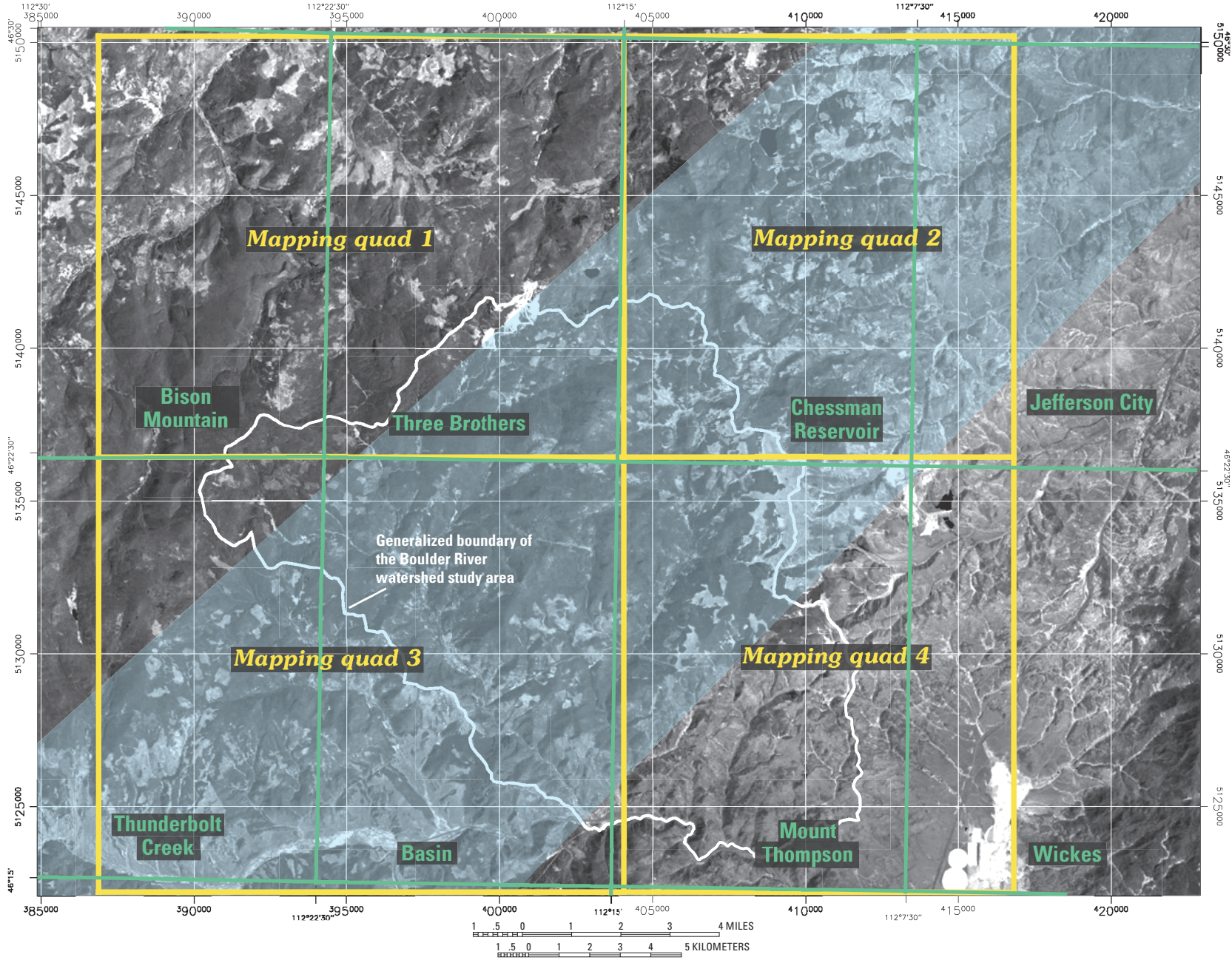


**Figure 6.** Site map showing USGS 7.5-minute quadrangle (1:24,000 scale) boundaries (green), linear feature mapping quads (yellow), and approximate area of the Butte-Helena fault zone (blue).

cell represents the total lengths, added together, of all linear features that pass through the cell. The total length of each linear feature is calculated, not just the length of the section of the feature that lies within the cell. In an intersection grid, the value for each cell represents the number of intersections of linear features that occur within the cell. Each contour map was made using a grid cell size of 2,500 ft on each side. This grid cell size was selected, based on the results of various test dimensions, to minimize false map features produced by the gridding algorithm.

Contour maps combining spatial frequency and intersection data, and spatial frequency and length data were produced to show where these features occur together. Values for linear feature spatial frequency, intersections, and length were normalized, that is, the values from each data set were divided by their maximum value so that all values would range from 0 to 1. The data were then combined to produce the values that were contoured in the combination maps. In terms of ground-water flow, areas with greater combined spatial frequency and intersections may identify where greater hydraulic connection in the bedrock aquifer exists, assuming fractures are hydraulically conductive. Areas where greater spatial frequency and linear feature length are coincident represent deeper ground-water circulation. Longer linear features likely represent fractures extending to greater depths, and therefore, deeper ground-water circulation, again assuming that the fractures are hydraulically conductive.

The contour map depicting linear feature spatial frequency and intersections was combined with a map of shallow ground water and wetland areas. This map is a derivative product from a land-type inventory of the Beaverhead-Deerlodge National Forest (D. Ruppert, unpub. data, 1980); it shows areas where ground water occurs at or near the land surface. Some of the water associated with areas of high water tables has been observed on the ground and on aerial photos as originating from seeps and springs oriented along linear features. These linear features are interpreted as being associated with bedrock structures. The purpose of combining these maps is to identify where zones of inferred high fracture frequency and areas where the potentiometric surface is close to the land surface coincide. These correlated areas may represent recharge to or discharge from fractured rock.

## Results and Analysis

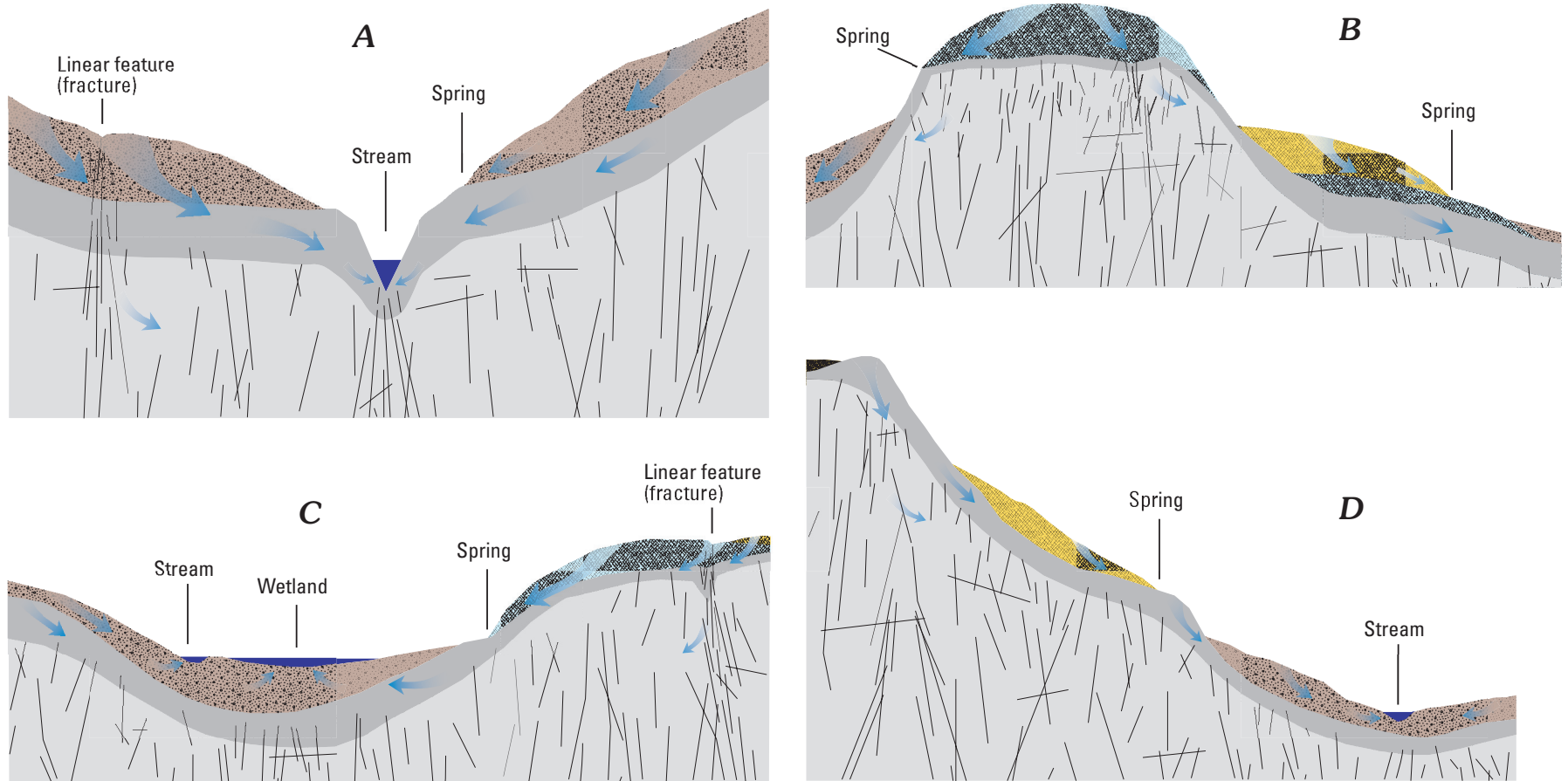
### Conceptual Model of Ground-Water Flow

Geologic units in the Boulder River watershed study area can be grouped, based on their relative hydraulic conductivity, into three hydrogeologic units that correspond to three layers of a conceptual ground-water flow model (fig. 7). The upper model layer represents unconsolidated deposits and has the largest hydraulic conductivity. The second model layer








represents the upper fractured and weathered zone in the granodioritic bedrock: it has a smaller hydraulic conductivity than the unconsolidated deposits but a much greater hydraulic conductivity than underlying unweathered Butte pluton. Fractured rocks of Elkhorn Mountains Volcanics and Tertiary volcanics also are included in the second model layer of rocks having intermediate hydraulic conductivity. The third or lowest layer of the conceptual model represents the very low hydraulic conductivity of the Butte pluton. The crystalline rocks are likely fractured at depth, but fracture permeability undoubtedly decreases with depth. The exception to this low permeability might occur in fault zones where hydraulic conductivity in fractures might increase. This three-layer conceptual model oversimplifies the hydraulic properties of rocks in the study area; however, it preserves important hydraulic characteristics, which are that hydraulic conductivity is greatest in the upper unconsolidated alluvium and generally decreases with depth. The hydrogeologic properties of the Butte pluton are the primary factors that limit development of regional ground-water flow systems in the study area.

Topography determines the upper geometry of the ground-water basin and is a major control on direction of ground-water flow in a basin such as the Boulder River watershed, where at depth no extensive high permeability unit exists. The steep hummocky terrain of the study area, combined with the decrease in hydraulic conductivity of geologic units with depth, results in the formation of mostly shallow, localized ground-water flow systems (Toth, 1963; Freeze and Witherspoon, 1967). Direction of shallow ground-water flow in the study area can be modeled as the gradient of topographic slope. Mathematical analysis (Freeze and Witherspoon, 1967) has shown that changes in topographic slope, combined with decreasing hydraulic conductivity with depth, will focus ground-water discharge at breaks in slope and at geologic contacts, similar to those observed in the Boulder River watershed. A conceptual three-layer model of decreasing hydraulic conductivity with depth also is consistent with the generally shallow depths to ground water observed in the study area. In the conceptual model of ground water just outlined, the upper layer of rocks has the greatest hydraulic conductivity and transports the greatest amount of ground water per unit volume of aquifer on an annual cycle. The second layer of rocks, having intermediate hydraulic conductivity, transports a smaller amount of ground water than the upper layer. The third layer of rocks, in which hydraulic conductivity is very low, transports the least amount of water annually, even though the amount of water stored within this unit may be large.

The ground-water flow regimes included in the conceptual model (fig. 7) are typical of conditions in the watershed; the views are meant to represent various settings for ground- and surface-water interaction and to depict the geologic controls on basin hydraulics. Figure 7A illustrates an area where principal recharge is through unconsolidated alluvium, with secondary recharge through surface fractures. Ground-water discharge in this flow regime is to springs that occur at the



**EXPLANATION**

-  Unconsolidated deposits (model layer 1 - high hydraulic conductivity)
  -  Fractured Lowland Creek Volcanics (model layer 2 - moderate hydraulic conductivity)
  -  Fractured Elkhorn Mountains Volcanics (model layer 2 - moderate hydraulic conductivity)
  -  Upper fractured or weathered zone of the Boulder batholith (model layer 2 - low to moderate hydraulic conductivity)
  -  Plutonic rocks of the Boulder batholith and intrusives (model layer 3 - low hydraulic conductivity)
  -  Various oriented faults, fractures, and joints
-  Direction of ground-water flow

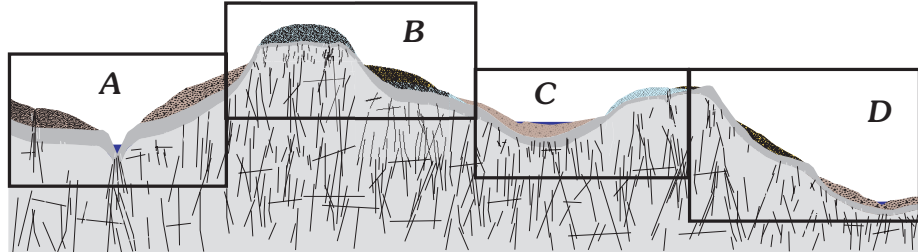


**Figure 7.** Conceptual ground-water model and depiction of flow regimes in the Boulder River watershed (cross sections are for purposes of illustration and are not to scale). Areas corresponding to views are noted in text.



contact between unconsolidated alluvium and plutonic rocks, and to a channel whose location was likely controlled by bedrock fractures. Cataract Creek near the confluence of Uncle Sam Gulch is an example of this type of stream.

Figure 7B illustrates a flow regime where ground-water recharge occurs at a topographic high, in fractured Elkhorn Mountains Volcanics (analogous to conditions at Jack Mountain), and in the fractured Lowland Creek Volcanics. Ground-water discharge in this regime is to springs at the contact between the Cretaceous and Tertiary volcanics, and the contact of the Elkhorn Mountains Volcanics and underlying plutonic rocks.

The flow regime in Figure 7C depicts ground-water recharge occurring in unconsolidated alluvium, fractured Elkhorn Mountains Volcanics, and throughgoing fractures in volcanic and plutonic rocks. Discharge is to wetlands and adjacent streams in glacial valley fill (analogous to Buckeye Meadows), and to springs that occur at breaks in slope and the contact between volcanic and plutonic rocks.

Figure 7D illustrates a ground-water flow regime where recharge occurs in exposed fractured and weathered plutonic rocks, fractured Lowland Creek Volcanics, and unconsolidated alluvium. Discharge in this regime is to springs located at the contact between Tertiary volcanics and plutonic rocks, and to streams in unconsolidated alluvium. Examples of this flow regime are the lower Basin Creek valley, upstream from the town of Basin, and upper Cataract Creek meadows.

## Linear Feature Analysis

Linear features were mapped within the Boulder River watershed study area and in areas surrounding the study area (fig. 8). A total of 563 features were mapped. These linear features are interpreted as representing the surface expression of faults, joints, other fractures, and mineralized veins. Statistical summaries of length and orientation are in tables 1 and 2. The mapped linear features range in length from 671 ft to 26,070 ft, with a mean of 4,902 ft. The mean orientation (azimuth) of all mapped features is  $79.92^\circ$ . The primary and secondary orientations and other minor trends of linear features are summarized in table 3.

A rose diagram summarizing the orientations of all mapped linear features is shown in figure 9A. Figure 9B has a similar rose diagram in which the orientations were weighted according to each feature's length. Both rose diagrams show two primary trend sets with azimuths of  $65^\circ$  and  $105^\circ$ . The length weighted rose diagram was compared to rose diagrams of lineament and fault orientation analysis results from a previous study (Smedes, 1966) of the northern Elkhorn Mountains (adjacent to and northeast of the area of this study). These diagrams show the orientation of 996 faults and 1,357 lineaments that were mapped from field observations and aerial photos, and weighted by length. The comparison with linear feature orientations (fig. 9B) shows a correlated trend of faults to the northeast, and of lineaments to the east-northeast. There

is little correlation in the prominent trend of fault orientation to the southeast. However, the average angle of illumination of the remote sensing base images, as described preceding, is co-linear with this trend, and linear features oriented in this direction would be less discernible.

The length filtered rose diagrams indicate that short to moderate-length linear features (fig. 10A and 10B) generally trend to the northeast and east-northeast. The moderate- to long length features, ranging from 3,280 to 26,250 ft (1,000 to 8,000 m) (fig. 10C and 10D) also have two primary trend sets, with a predominant orientation to the east-southeast and a secondary orientation to the east-northeast.

The mapped lineaments grouped by quadrant (fig. 11A–D) have a consistent east-west primary mean azimuth direction similar to that seen in the length filtered rose diagrams. The primary and secondary orientations in the quadrant-grouped diagrams are typically about  $100^\circ$ – $110^\circ$  and  $70^\circ$ – $80^\circ$ . A minor orientation in figure 11A and 11C is  $20^\circ$ – $30^\circ$ , and in figure 11D is  $30^\circ$ – $40^\circ$ . In a previous study of the Jefferson City 15-minute quadrangle (Becraft and others, 1963), a northeast primary trend of nonmineralized faults and topographically expressed lineaments (fig. 11E) was observed. Minor trends are at  $0^\circ$ – $10^\circ$ ,  $90^\circ$ – $100^\circ$ , and  $140^\circ$ – $150^\circ$ . The Jefferson City 15-minute quadrangle corresponds to the eastern part of this study (quadrants 2 and 4, fig. 6). In order to compare trends from the same area, linear features from quadrants 2 and 4 were combined and the rose diagram from Becraft and others (1963) was overlaid (fig. 11E). There are correlated trends to the northeast and east, and to a lesser extent, to the southeast. The trend at  $0^\circ$ – $10^\circ$  shown in the rose diagram from Becraft and others (1963) is not well correlated.

Mapping quadrant 1 (fig. 6) covers an area corresponding with a portion of the laccolithic western part of the Boulder batholith, northwest of the Butte-Helena fault zone (O'Neill and others, this volume, fig. 16). Part of the area is overlain with Elkhorn Mountains Volcanics. Mapping quadrant 4 is southeast of the Butte-Helena fault zone and includes areas of the Butte pluton, Elkhorn Mountains Volcanics, and Lowland

**Table 1.** Summary statistics for mapped linear features.

Mean	4,902 ft
Standard error	157 ft
Median	3,600 ft
Mode	3,678 ft
Standard deviation	3,713 ft
Range	25,400 ft
Minimum	671 ft
Maximum	26,070 ft
Sum	2,759,538 ft
Count	563

**Table 2.** Summary statistics for orientations of mapped linear features.

[--, when length filtering is deactivated, minimum and maximum length are not applicable]

Rose diagram	Calculation method	Length filtering	Minimum length (feet)	Maximum length (feet)	Sample size	Maximum percentage	Mean percentage	Mean azimuth (degrees)	Relative standard deviation (percent)	Confidence interval (degrees)	R-magnitude
fig. 9A	Frequency	Deactivated	--	--	563	13.3	5.6	79.92	3.54	3.13	0.80
fig. 9B	Length	Deactivated	--	--	563	18.3	5.6	83.79	4.51	3.03	0.81
fig. 10A	Length	Activated	3.3	1,640	51	15.9	7.7	63.20	5.06	8.90	0.85
fig. 10B	Length	Activated	1,640	3,281	192	11.6	5.6	77.17	3.56	5.33	0.80
fig. 10C	Length	Activated	3,281	9,843	264	15.8	5.9	84.32	3.31	4.82	0.78
fig. 10D	Length	Activated	9,843	26,247	56	30.3	9.1	88.32	9.27	7.20	0.89
fig. 11A Quadrant 1	Frequency	Deactivated	--	--	196	12.8	5.6	74.30	3.65	5.57	0.78
fig. 11B Quadrant 2	Frequency	Deactivated	--	--	150	18.7	5.6	85.55	5.14	5.20	0.85
fig. 11C Quadrant 3	Frequency	Deactivated	--	--	99	16.2	5.9	79.90	3.82	8.27	0.76
fig. 11D Quadrant 4	Frequency	Deactivated	--	--	118	14.4	5.9	81.72	3.80	6.64	0.81

**Table 3.** Summary of main orientations of mapped linear features.

	<b>Mean azimuth (degrees)</b>	<b>Primary orientation (degrees)</b>	<b>Secondary orientation (degrees)</b>	<b>Other minor trends (degrees)</b>
All linear features	79.92	100-110	70-80	20-30
All linear features weighted by length.	83.79	100-110	70-80	30-40
Length filtered				
3.3-1,640 ft (1-500 m)	63.20	20-40	50-60	70-80
1,640-3,281 ft (500-1,000 m)	77.17	60-70	90-110	20-30
3,281-9,843 ft (1,000-3,000 m)	84.32	100-110	60-80	30-40
9,843-26,247 ft (3,000-8,000 m)	88.32	90-110	60-70	30-40
Grouped by quadrant				
Quadrant 1 (NW)	74.30	100-110	70-80	20-30
Quadrant 2 (NE)	85.55	100-110	60-80	130-140
Quadrant 3 (SW)	79.90	90-100	20-30	50-80
Quadrant 4 (SE)	81.72	70-80	100-120	30-40

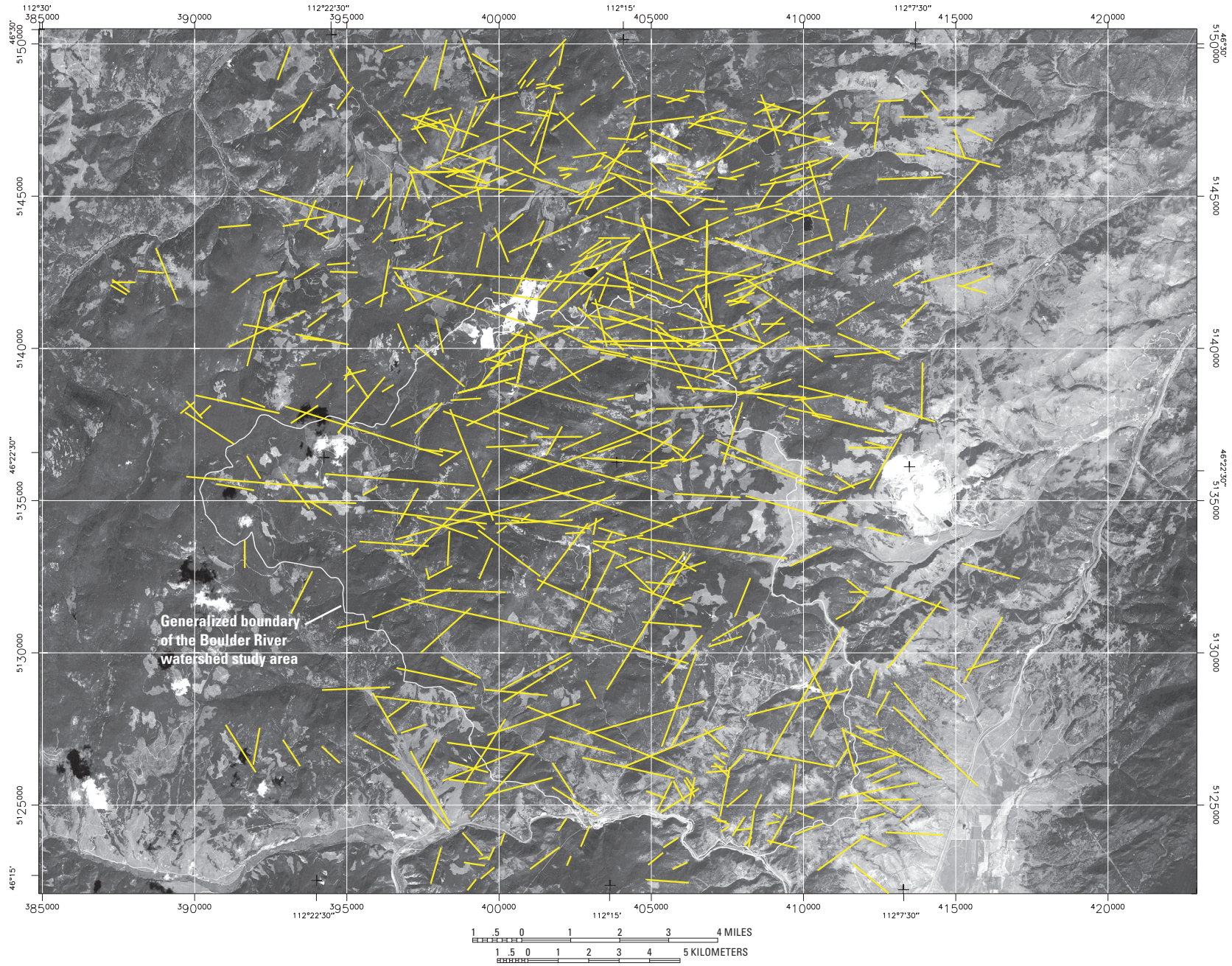
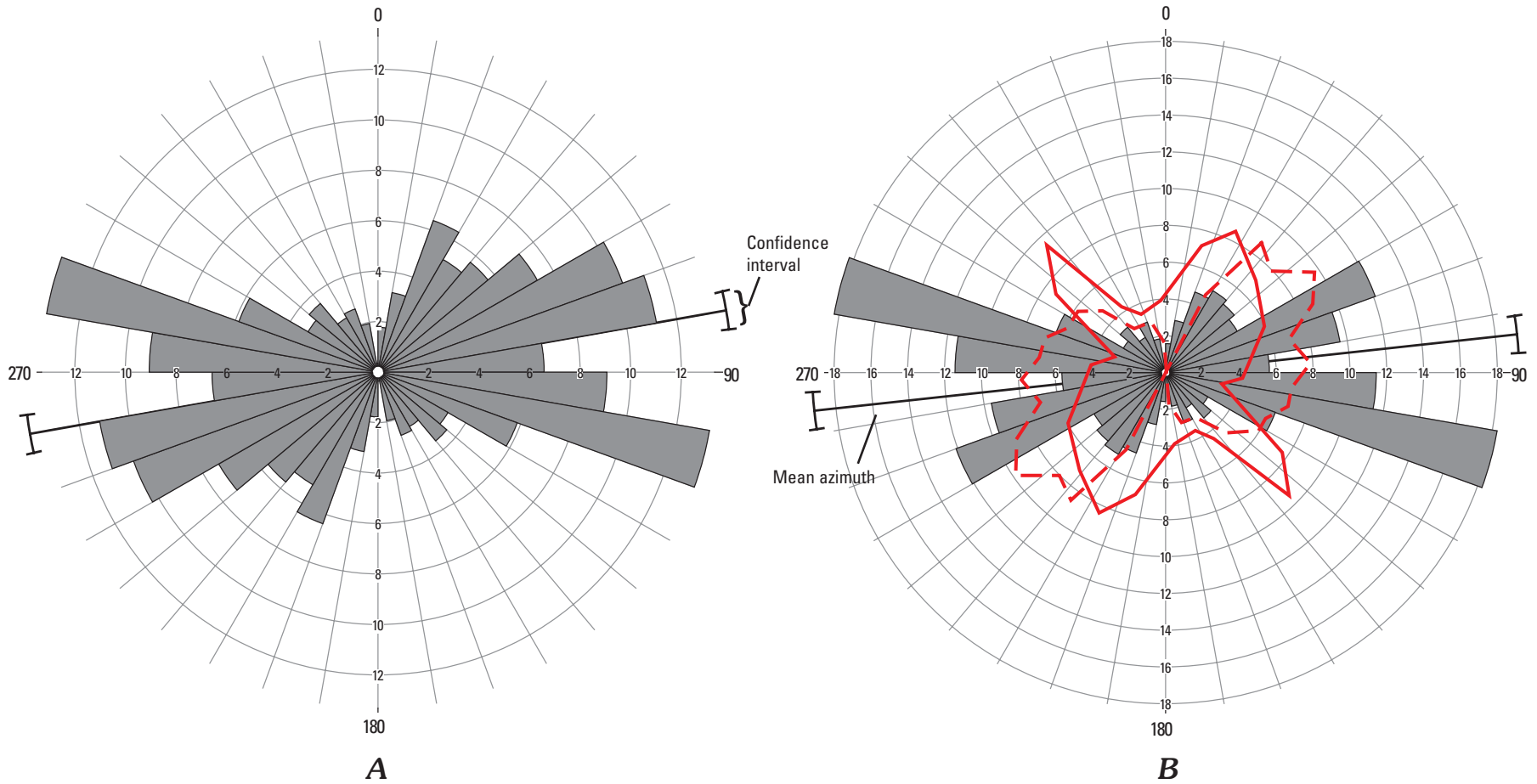
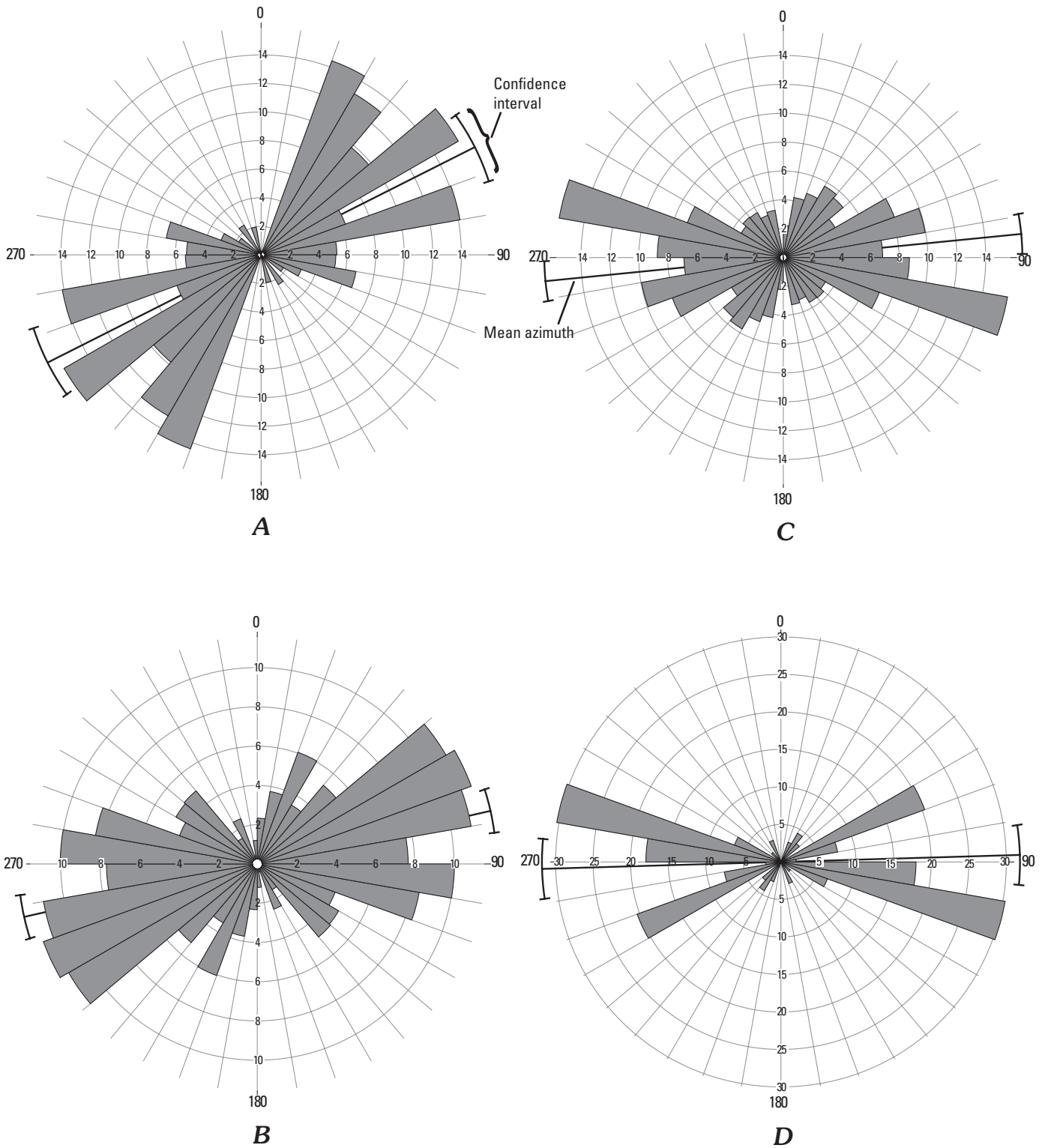


Figure 8. Mapped linear features, Boulder River watershed study area and adjacent region.



**Figure 9.** Rose diagrams representing *A*, orientations of all linear features, and *B*, all linear features weighted by length. The confidence interval represents the interval on either side of the mean azimuth that most likely (using a 95 percent confidence level) contains the true mean direction. Rose diagrams from a previous study (Smedes, 1966) of the northern Elkhorn Mountains showing the orientation of 996 faults (solid red line) and 1,357 lineaments (dashed red line) are shown in view B.



**Figure 10.** Length filtered rose diagrams of linear features *A*, 3.3–1,640 ft (1–500 m) in length; *B*, 1,640–3,281 ft (500–1,000 m) in length; *C*, 3,281–9,843 ft (1,000–3,000 m) in length; *D*, 9,843–26,247 ft (3,000–8,000 m) in length. The mean azimuth and confidence interval are shown for each diagram.

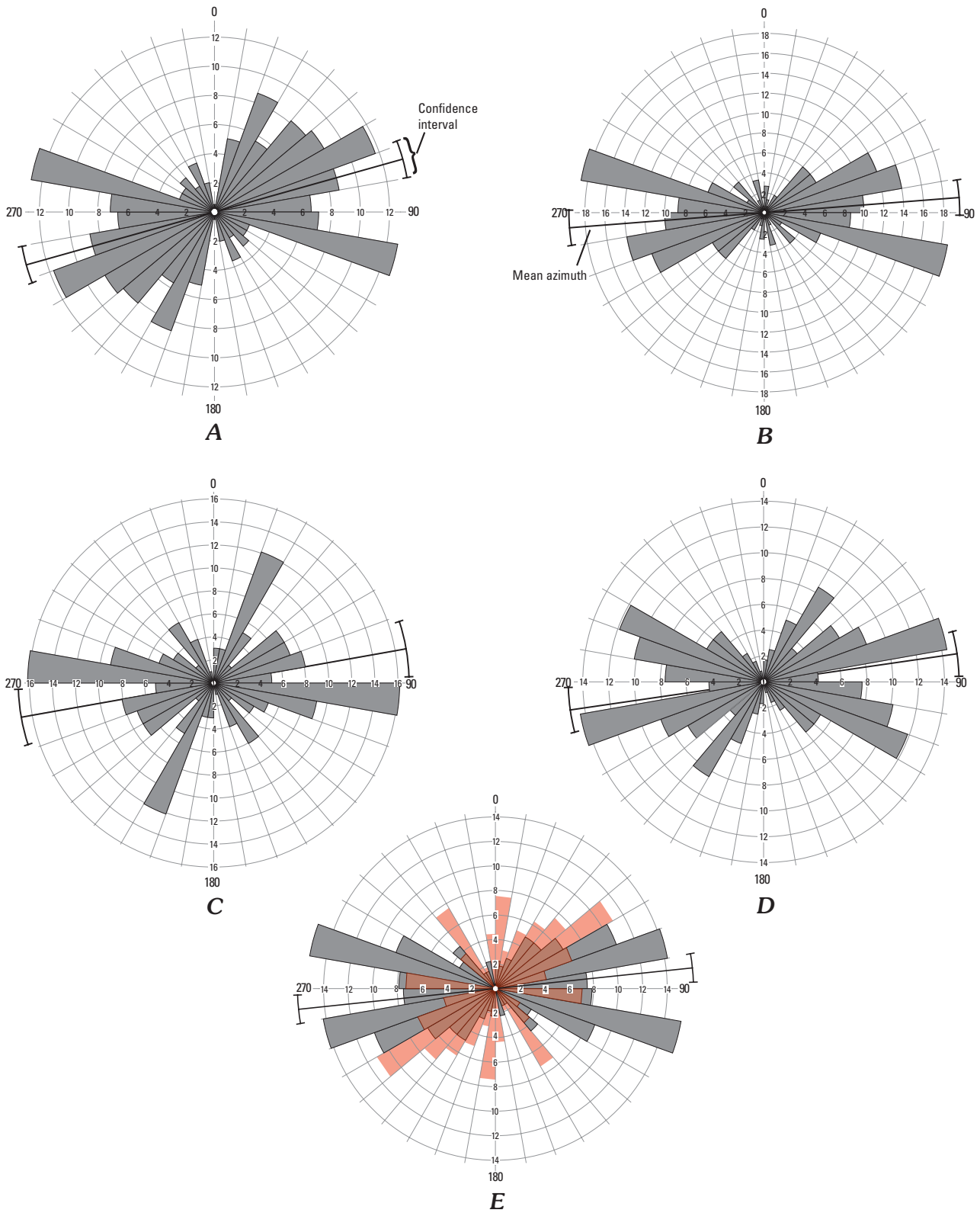


**Figure 11.** Rose diagrams showing linear feature orientation arranged by quadrants shown in figure 6. *A*, quadrant 1; *B*, quadrant 2; *C*, quadrant 3; *D*, quadrant 4. The mean azimuth and confidence interval are shown for each diagram. *E*, rose diagram (red) from a previous study (Becraft and others, 1963) in the Jefferson City 15-minute quadrangle of the trends of 142 nonmineralized faults and topographically expressed lineaments overlaid on combined linear feature orientation of quadrants 2 and 4.

Creek Volcanics. The trends of mapped linear features for these two quadrants are similar (fig. 11A and 11D), with the exception of a minor trend oriented to the north-northwest in quadrant 1. The similarity of linear feature orientation in these two quadrants suggests a consistent pattern of fracturing north-west and southeast of the Butte-Helena fault zone.

Quadrant 2 and quadrant 3 (fig. 6) represent the north-eastern and southwestern portion, respectively, of the Butte-Helena fault zone within the study area. Linear features in the northeast quadrant (fig. 11B) show two primary trend sets similar to the orientation of spatial frequency distribution for the entire study area (fig. 9A). The southwest quadrant (fig. 11C) has primary east-west ( $90^{\circ}$ – $100^{\circ}$ ) and north-northeast ( $20^{\circ}$ – $30^{\circ}$ ) orientations, with minor classes trending east-northeast ( $50^{\circ}$ – $80^{\circ}$ ) and southeast ( $140^{\circ}$ – $160^{\circ}$ ). These orientation classes are consistent with the synemplaced diastrophic fracture orientations of the Butte pluton (O'Neill and others, this volume). Because of the more dispersed orientations in this quadrant, fracture-controlled ground-water flow directions would also be expected to be more diffuse.

Within the Boulder River watershed study area, the greatest occurrence of linear feature spatial frequency, length, and intersection frequency (figs. 12–14) was mapped near the Continental Divide at the northern boundary of the study area between Old Baldy and Lava Mountains. Other areas of high linear feature spatial frequency are indicated in the central part of the watershed near the Crystal mine, in the north part of the watershed near the Buckeye mine, and in the south part of the watershed east of Basin (fig. 12). Longer linear features also occur in the central part of the watershed near the Crystal and Bullion mines and in the southern part of the watershed (fig. 13). Combined contour maps of linear feature spatial frequency and intersections (fig. 15), and spatial frequency and length (fig. 16) show similar results, with an area of high combined spatial frequency and length west of the Bullion mine.

Areas of relatively dense linear features overlap with areas of mapped shallow ground water (fig. 17) in several locations. An instance is seen in the northern part of the watershed between Old Baldy Mountain and Lava Mountain. Old Baldy Mountain is mapped as an area of high linear feature spatial frequency and is flanked on the east and south by areas where the water table is near the land surface. Similar occurrences of this correlation are seen in the central part of the watershed near the Crystal and Bullion mines, and in the northwest part of the study area near Basin Creek. Areas of high linear feature spatial frequency on either flank of the Continental Divide and in other topographically high areas likely have enhanced ground-water recharge through the fractures in volcanic and plutonic rocks. Adjacent areas of inferred shallow ground water represent potential discharge in unconsolidated alluvium, fractured volcanics, and fractured plutonic rocks.

## Conclusions and Discussion

Based on field observations at the Buckeye, Bullion, and Crystal mines and the ground-water flow concepts outlined here, ground-water flow to mines in the Boulder River watershed study area is primarily local in origin. Ground-water flow to underground workings, such as those at the Bullion and Crystal mines, primarily comes from infiltration of shallow ground water from rocks above the mine workings and from interception of surface runoff into mine trenches and pits. Ground water that enters mine workings through lateral flow from fractured plutonic rocks is a relatively small percentage of the total water entering mines. Remediation efforts that eliminate ponded surface water near mine workings and reduce infiltration and surface runoff to caved adits and trenches would significantly reduce the quantity of shallow ground water entering mine workings. The relatively small amount of ground water that enters underground mine workings from deeper fractures in plutonic rocks probably could not be eliminated or even significantly reduced through any surface remediation efforts. Given the probable long residence times for deep circulation and relatively high acid-neutralizing potential (Desborough and others, 1998) of the plutonic rocks, fracture-controlled ground water at depth likely would not adversely affect surface water quality in the watershed.

The primary surface-water flow direction (Basin Creek, Cataract Creek, and High Ore Creek) in the watershed is to the south into the Boulder River. Shallow ground water in the unconsolidated aquifer likely follows a similar flow direction, which is primarily topographically controlled. However, the predominant east-west orientation, and the orientation of other minor trends, of mapped linear features, assumed associated with fractures, may have a significant influence on structurally controlled shallow ground-water flow directions. The orientation of bedrock linear structural features likely affects the flow direction of deeply circulating regional ground-water flow. The rose diagrams presented in this study indicate that the orientations of mapped linear features at the surface are co-linear with the orientation of geophysical gradients in the subsurface (McCafferty and others, this volume). This suggests that some linear structures extend to considerable depth, and that ground-water storage at depth is potentially large.

The high linear feature frequency indicated in areas along the Continental Divide is significant in that these areas represent potential recharge to fracture-controlled ground water in both the Boulder River watershed and the Tenmile Creek watershed to the north. The higher occurrence of mapped linear features could identify potential recharge sources for fracture-controlled ground water, consistent with the conceptual model presented in this study.

The results of this study provide a conceptual understanding of the ground-water and surface-water relationships in the watershed, identify possible fracture-controlled ground-water recharge areas associated with near-surface structures, and map areas of greatest linear feature spatial frequency. These components should be considered in any mine-site restoration strategy or in identifying suitable locations for mine-waste repositories.



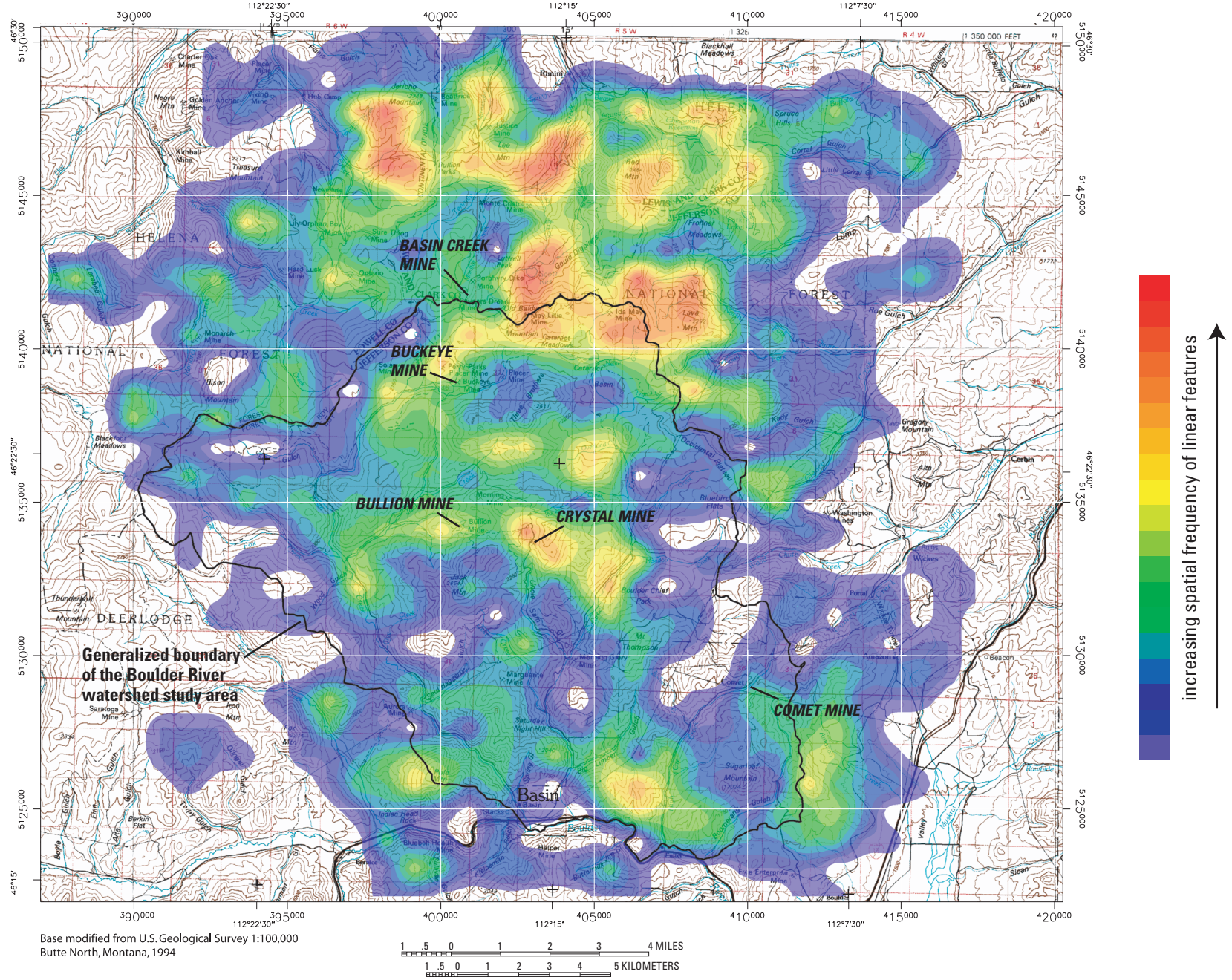
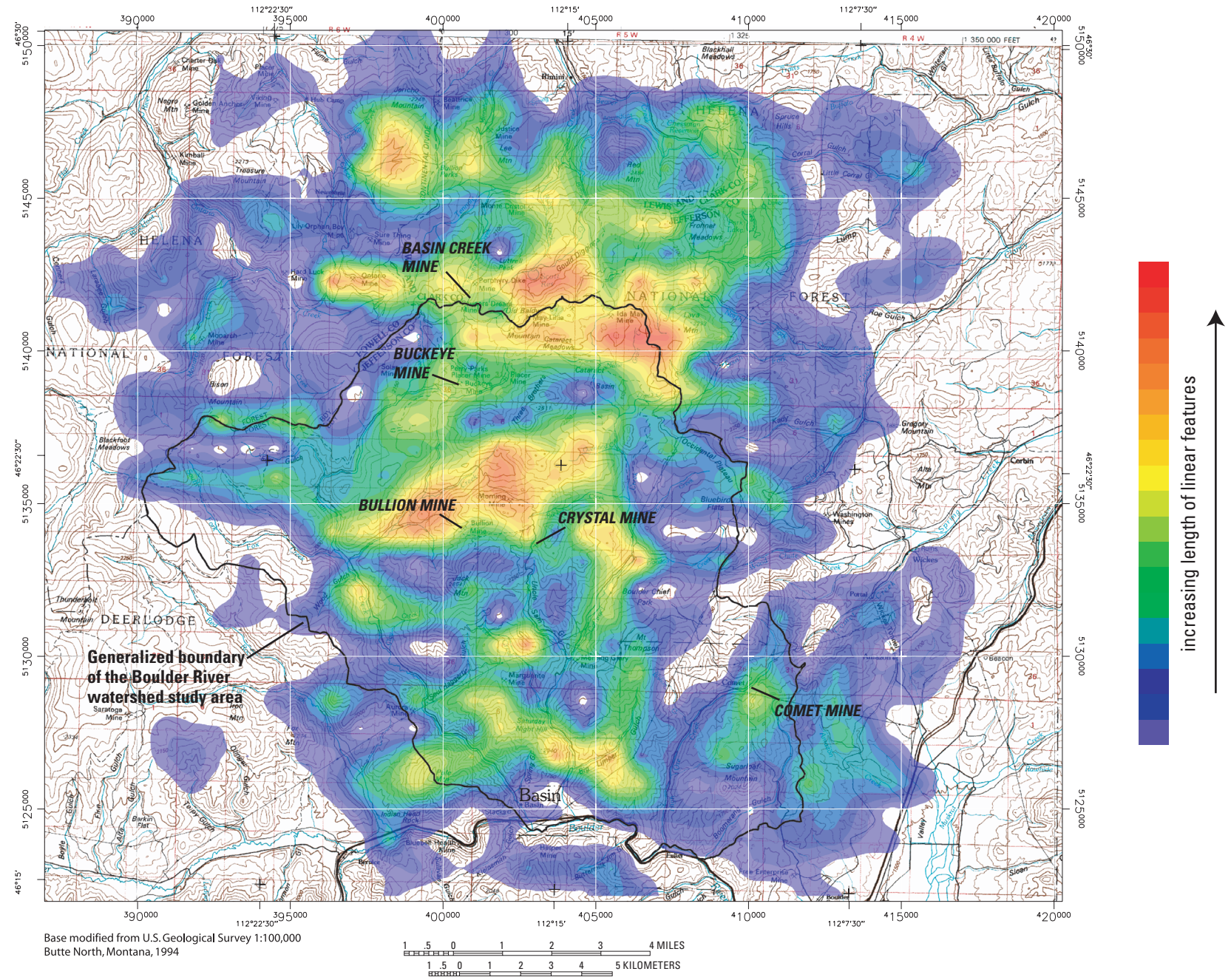


Figure 12. Contour map of linear feature spatial frequency (2,500 ft grid cell size) in the Boulder River watershed region.



Base modified from U.S. Geological Survey 1:100,000 Butte North, Montana, 1994

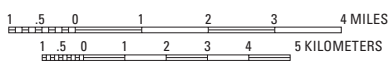


Figure 13. Contour map of linear feature length (2,500 ft grid cell size) in the Boulder River watershed region.

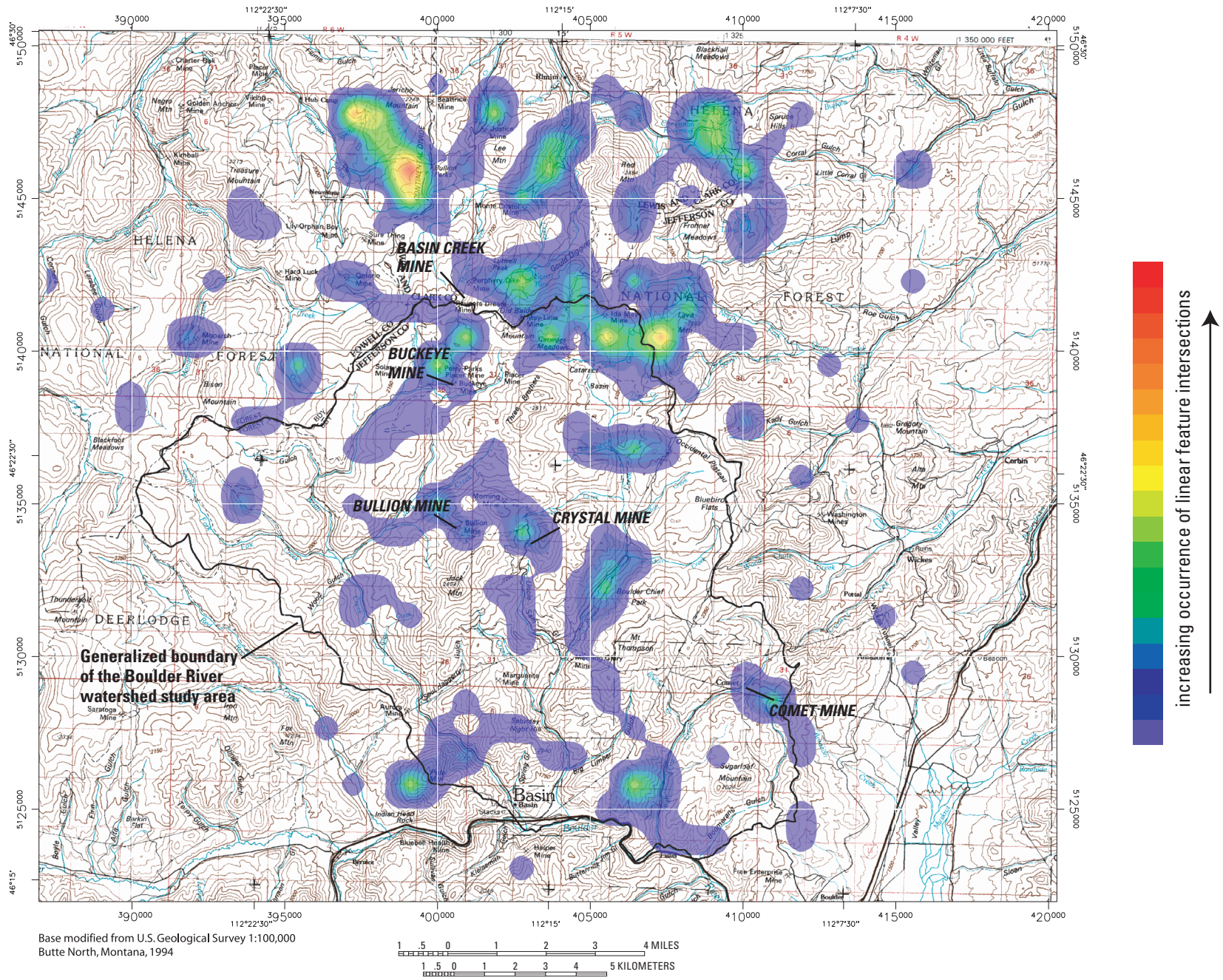
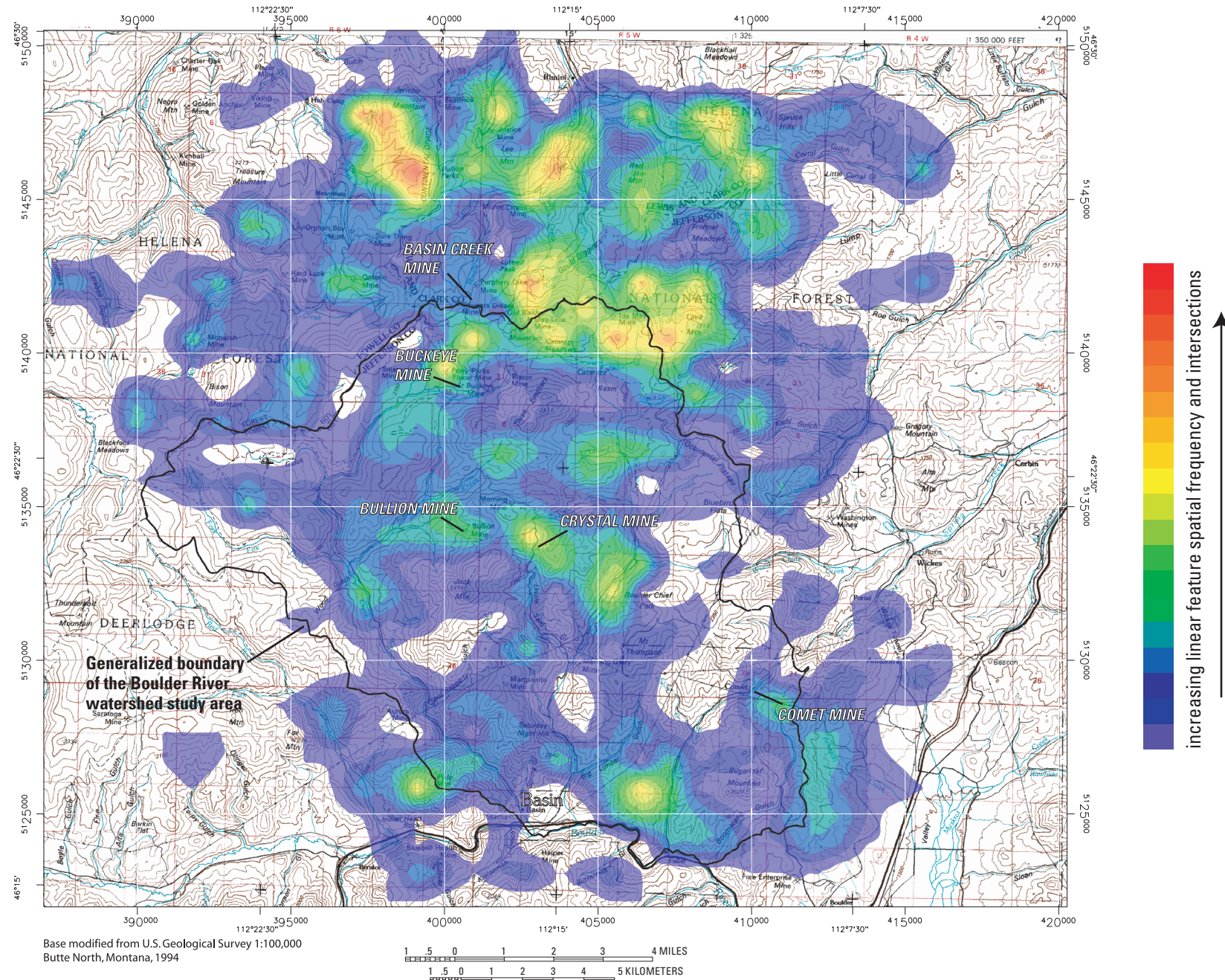


Figure 14. Contour map of linear feature intersections (2,500 ft grid cell size) in the Boulder River watershed region.



**Figure 15.** Contour map of combined linear feature spatial frequency and intersections (2,500 ft grid cell size) in the Boulder River watershed region.

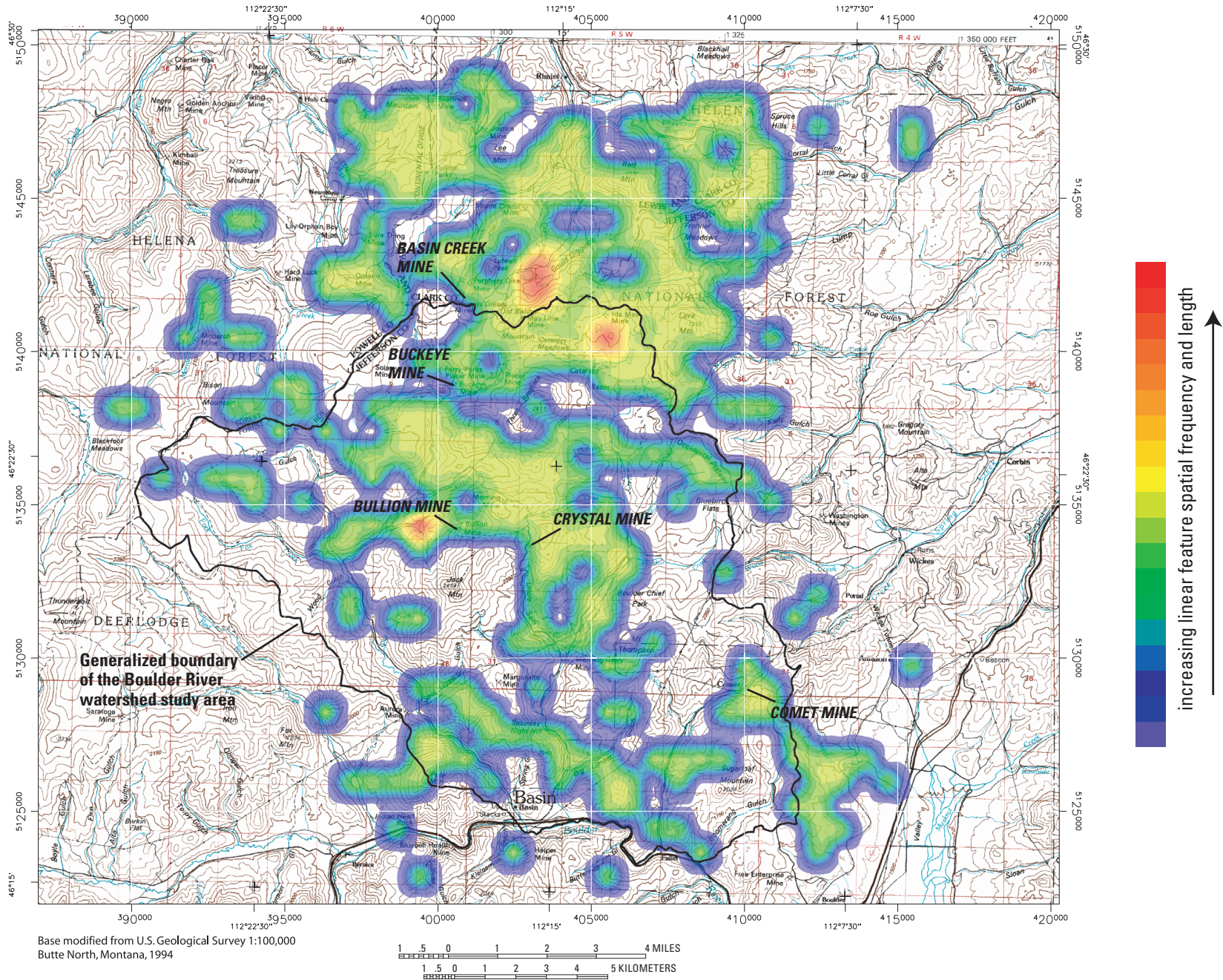
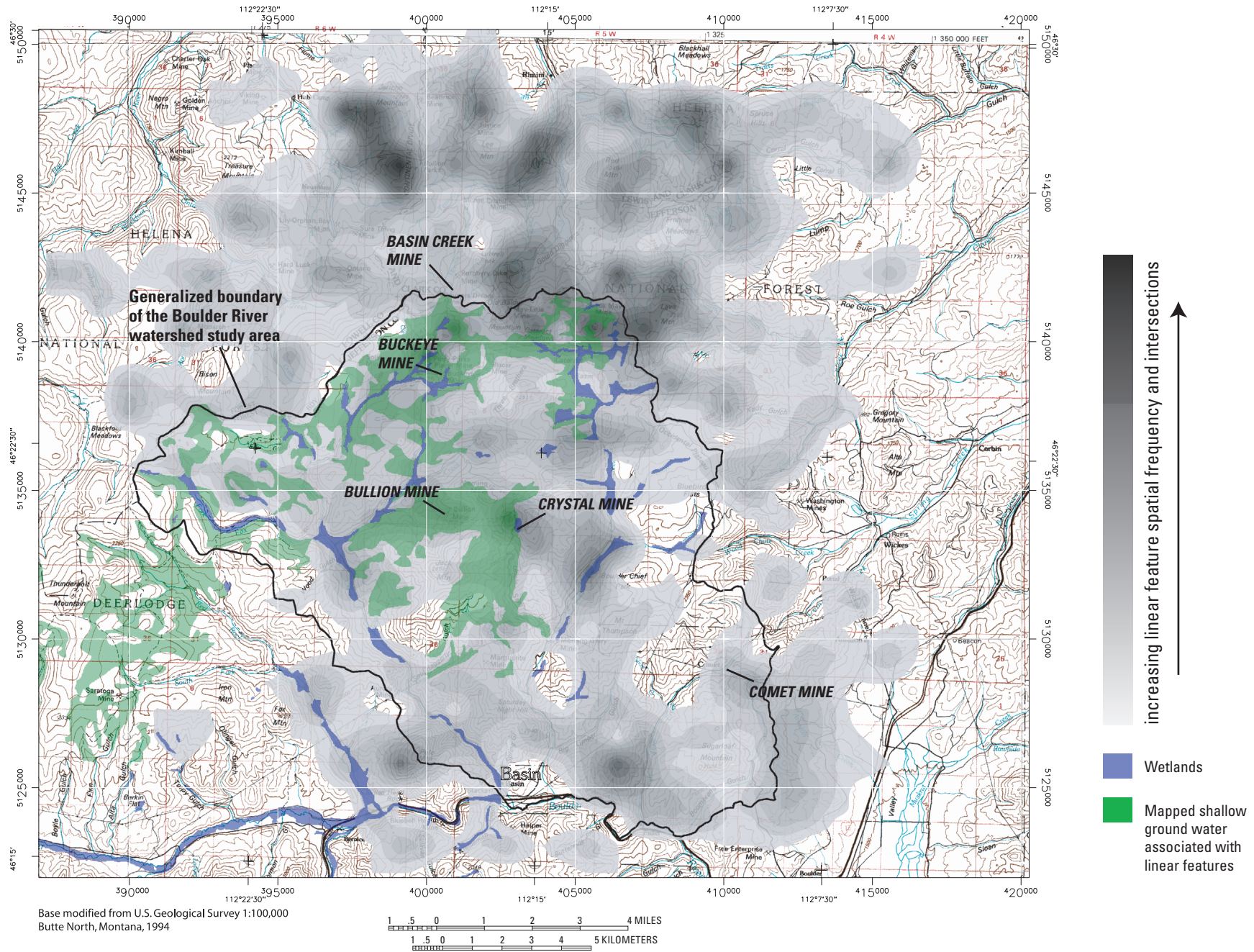


Figure 16. Contour map of combined linear feature spatial frequency and total length (2,500 ft grid cell size) in the Boulder River watershed region.



**Figure 17.** Contour map of combined linear feature spatial frequency and intersections, and areas of mapped shallow ground water (2,500 ft grid cell size).

## References Cited

- Becraft, G.E., Pinckney, D.M., and Rosenblum, Sam, 1963, Geology and mineral deposits of the Jefferson City quadrangle, Jefferson and Lewis and Clark Counties, Montana: U.S. Geological Survey Professional Paper 428, 101 p., 18 plates.
- Desborough, G.A., Briggs, P.H., and Mazza, N., 1998, Chemical and mineralogical characteristics and acid-neutralizing potential of fresh and altered rocks and soils of the Boulder River headwaters in Basin and Cataract Creeks of Northern Jefferson County, Montana: U.S. Geological Survey Open-File Report 98-40, 21 p.
- Eliason, E.M., and McEwen, A.S., 1990, Adaptive box filters for removal of random noise from digital images: *Photogrammetric Engineering & Remote Sensing*, v. 56, no. 4, p. 453.
- Freeze, R.A., and Cherry, J.A., 1979, *Groundwater*: Englewood Cliffs, N.J., Prentice-Hall, Inc., 604 p.
- Freeze, R.A., and Witherspoon, P.A., 1966, Theoretical analysis of regional groundwater flow—I, Analytical and numerical solutions to the mathematical model: *Water Resources Research*, v. 2, no. 4, p. 641–656.
- Freeze, R.A., and Witherspoon, P.A., 1967, Theoretical analysis of regional groundwater flow—II, Effect of water table configuration and subsurface permeability variation: *Water Resources Research*, v. 3, no. 2, p. 623–634.
- Hubbert, M.K., 1940, The theory of ground-water motion: *Journal of Geology*, v. 48, no. 8, pt. I, p. 785–944.
- Isaaks, E.H., and Srivastava, R.M., 1989, *An introduction to applied geostatistics*: New York, Oxford, 561 p.
- Knepper, D.H., 1996, Interpreted linear features from Landsat Thematic Mapper images, Southern Ute Indian Reservation, Colorado, *in* *Geology and resources of the Paradox Basin, Utah*: Utah Geological Association Guidebook 25.
- Maxim Technologies Inc., 1999, Final engineering evaluation of potential repository sites, Beaverhead-Deerlodge and Helena National Forests, Lewis and Clark, Powell, and Jefferson Counties, Montana: Helena, Mont., prepared for USDA Forest Service, Region I, Missoula, Mont., variously paged.
- Research Systems, Inc., 1998, Boulder, Colorado, ENVI, The Environment for Visualizing Images.
- Rockware, Inc., 1999, Golden, Colorado, RockWorks99.
- Rowan, L.C., and Wetlaufer, P.H., 1975, Iron-absorption band analysis for the discrimination of iron-rich zones: U.S. Geological Survey, Type III Final Report, Contract S-70243-AG.
- Ruppel, E.T., 1963, Geology of the Basin quadrangle, Jefferson, Lewis and Clark, and Powell Counties, Montana: U.S. Geological Survey Bulletin 1151, 121 p., 7 plates.
- Sabins, F. F., 1987, *Remote sensing principles and interpretation*, Second Edition: New York, Freeman.
- Smedes, H.W., 1966, Geology and igneous petrology of the northern Elkhorn Mountains, Jefferson and Broadwater Counties, Montana: U.S. Geological Survey Professional Paper 510, 116 p.
- Toth, J., 1963, A theoretical analysis of groundwater flow in small drainage basins: *Journal of Geophysical Research*, v. 68, no. 16, p. 4795–4812.